PART II SURVEY RESULTS

CHAPTER 1 OUTLINE OF THE GEOLOGY OF THE AREA

1-1 Stratigraphy

The general stratigraphy of the area is shown in Fig.II-1-1. The geology of the South Batinah Coast area is mainly composed of Samail Ophiolite, Supra-ophiolite Sediments of Batinah Olistostrone, Tertiary and Quaternary sediments.

The Samail Ophiolite in the surveyed area consists of Sheeted-dyke Complex (SD), Samail Volcanic Rocks (SV) , Intrusive Rocks (I') as well as Batinah Olistostrone and Tertiary and Quaternary sediments.

1-1-1 Sheeted-dyke Complex (SD)

In outcrops, the Sheeted-dyke Complex appears as a set of sub-parallel dykes of 0.5 to 3m wide whose composition ranges from microgabbroic to doleritic. The Sheeted-dyke Complex grades upward into the Lower Volcanic Rocks.

1-1-2 Samail Volcanic Rocks (SV)

The Samail Volcanic Rocks can be divided into three members consisting of Lower Volcanic Rocks (SV1), Middle Volcanic Rocks (SV2) and Upper Volcanic Rocks (SV3).

(1) Lower Volcanic Rocks (SV1)

The Lower Volcanic Rocks consist of Lower extrusives rocks (V1-1), Upper extrusives rocks (V1-2) and metalliferous sediments (U1).

V1-1 consists of differential basaltic to andesitic lavas, and composed mainly of reddish brown colored pillow lava with large pillow size of 1m to 2m in diameter. V1-1 also consists of reddish brown to grey colored massive lava, hyaloclastite and pillow breccia. Characteristically, the pillow lava is aphanitic and accompanied with thick interpillows of 5cm to 40cm in thickness. The massive lava shows grey to brownish grey color with a thickness of several tenth centimeters to several meters. Columnar joints are developed in the thick massive lava.

V1-2 consists of primitive basaltic lava composed mainly of pillow lava accompanied with massive lava. The pillow lava shows light grey to purplish grey in color with pillow sizes mainly of 10cm to 1m in diameter and a maximum of 1.5m. It is characteristically accompanied with small sized pillow lavas of 10cm to 30cm in many places. Additionally, this pillow lava is porphyritic and shows a variole-like texture. In contrary V1-1 is accompanied with thin interpillows of 1cm to 5cm in thickness. The upper part of V1-2 includes pillow lavas with radial joints.

U1 is the so-called umber that includes many radiolarias and predominant in iron oxides. This unit

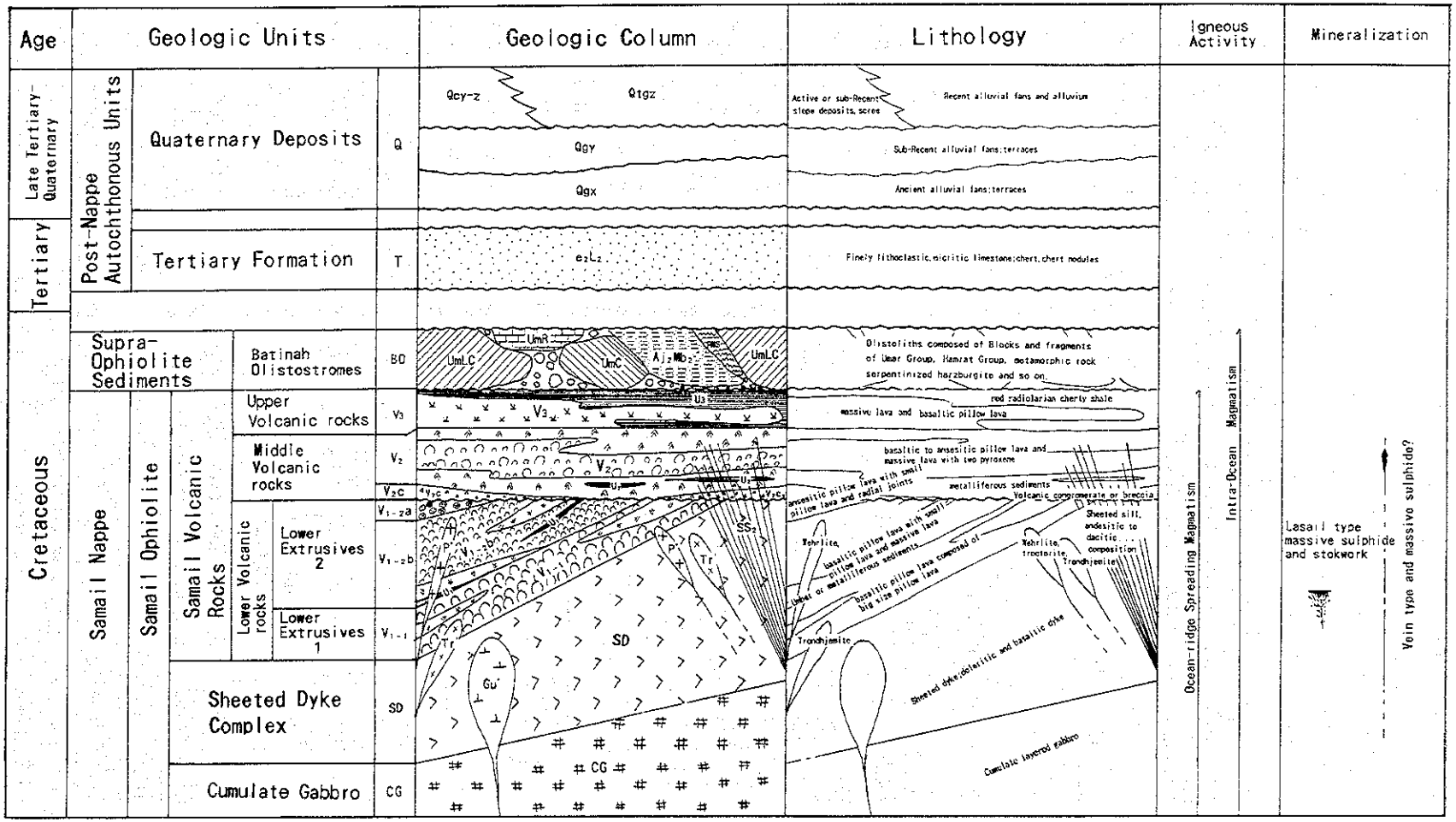

Fig. II-1-1 Stratigraphic columnar section of survey area

shows dark brown color.

(2) Middle Volcanic Rocks (SV2)

The Middle Volcanic Rocks (SV2) consist of volcanic conglomerates and breccia (V2c), extrusives rocks (V2) and metalliferous sediments (U2).

V2c consists of angular to rounded matrices of sand to gravels and of fragments and blocks of Sheeted dykes and Lower Volcanic Rocks.

V2 consists mainly of pillow lavas and massive lavas of andesite containing clinopyroxene and orthopyroxene. Most of the lavas are massive. The weathered surface shows various colors of grey, brownish grey, green, bluish grey and orange color. In general the massive lava shows a doleritic texture. The pillow lavas show purple, green and greenish grey colors. Most of the pillow lavas present irregular pillow shapes with diameters of about 0.5 to 1.0m.

U2 are the so-called umber and contains more radiolarias but fewer amounts of iron oxides than U1. This unit shows brownish black color.

(3) Upper Volcanic Rocks (SV3)

The Upper Volcanic Rocks consist mainly of extrusives rocks (V3) and metalliferous sediments (U3).

V3 is composed of doleritic massive lava (sheet flow) and pillow lava. Massive lava of V3 shows a light greenish grey color and forms a columnar joint in many places. The sheet flow of this massive lava reaches 170m in maximum thickness as one unit. Pillow lava of V3 can be seen in the lowermost, middle and uppermost of SV3, showing in general a dark greenish color. The size of pillows range mostly between 0.6m to 1.2m in diameter.

U3 is interbedded in the uppermost and middle parts of SV3. It is mainly composed of reddish brown sediments predominant in iron materials and accompanied with pinkish shale and jasper.

(4) Intrusive Rocks (I')

The Intrusive Rocks include peridotite (P'), gabbro (Gu'), trondhjemite (Tr') and late dolerite dykes. Peridotite (P') consists of wehrlite, troctolite, plagioclase-bearing dunite and olivine-bearing pyroxenite. Gabbro (Gu') is associated with diorite and quartz diorite. Trondhjemite (Tr') also includes quartz diorite in parts. Late dolerite dykes are accompanied with fine-grained gabbro.

1-1-3 Supra-ophiolite Sediments (Batinah Olistostrome)

The sediments (BO) consist of olistoliths of sedimentary formations formed in Tethys Sea. Olistoliths, which came as result of the obduction process at the same time when Tethys Sea closed, are composed of sedimentary and igneous rocks of Triassic to Cretaceous age.

1-1-4 Post-nappe autochthonous units

These units consist of Tertiary and Quaternary sediments. The Tertiary sediments consist of yellow

marl with large foraminifera (e2M1), upper nodular limestone (e2L2) and sedimentary breccia (Br) of late Paleocene to early Eocene. The Quaternary deposits consist of ancient alluvial fans (Qgx), sub-Recent alluvial fans (Qgy), active or sub-Recent slope deposits (Qcy-z), Khagra depressions with Recent or sub-Recent clay and silt (Qky-z), eolian sand of Recent or sub-Recent dunes (Qdy-z), coating of sub-Recent dunes (Qsy-z) and Recent alluvial fans and alluvium (Qtgz).

1-2 Geological Structure

Main structure in the South Batinah Coast area is the pile-up structure formed when allochthonous Samail Ophiolite and Supra-ophiolite sediments had been thrust over the Arabian shield at the late Cretaceous age. The Tertiary and Quaternary sediments of the post-nappe autochthonous units unconformably overlie the allochthonous units in the South Batinah Coast area. Many thrust faults are developed in the area that formed contacts of piled-up blocks originated before Tertiary and sliced the autochthonous and allochthonous blocks. High-angle faults developed in the area cut each of the above blocks and displaced the geological boundaries. These faults were formed before Tertiary.

1-3 Geology and Mineralization of the Surveyed Areas

Geological maps for the surveyed areas of Ghuzayn, Zuha, Maqail and Salahi are indicated respectively in the Figs. II-1-2, II-1-3, II-1-4 and II-1-5.

1-3-1 Ghuzayn Area

The geology of Ghuzayn area consists mainly of SD, V1-1, V1-2, U1, and V2 of Samail Ophiolite and Quaternary sediments.

Within this area a large scaled siliceous gossan is found with an approximate extension of 100m by 200m. An oxidized mineralized zone of disseminations and stockwork consisting of pyrite and chalcopyrite forms this gossan. Nearby the gossan are also found copper oxides and U1 with abundant magnetite.

In the south of Ghuzayn area it is observed U1 with abundant magnetite and copper oxides, while in the west it is found a silicified zone with scattered copper. In the west it can be found chalcopyrite bearing quartz veins and U1 with copper oxides.

1-3-2 Zuha Area

Zuha area is in the northern most part of the South Batinah Coast project area and located 35km west of Saham City. This area covers both of the mineral showings in Zuha and Zuha North.

As indicated in Fig.II-1-3, the geology consists mainly of V1-1, V1-2, U1, V2, U2 and Quaternary sediments. V1-2 outcrops in the central and southern parts of the area, namely, around the Zuha mineral showing. However, V1-2 is not exposed in the northern part because V1-1 is directly overlaid by V2 around the Zuha North mineral showing.

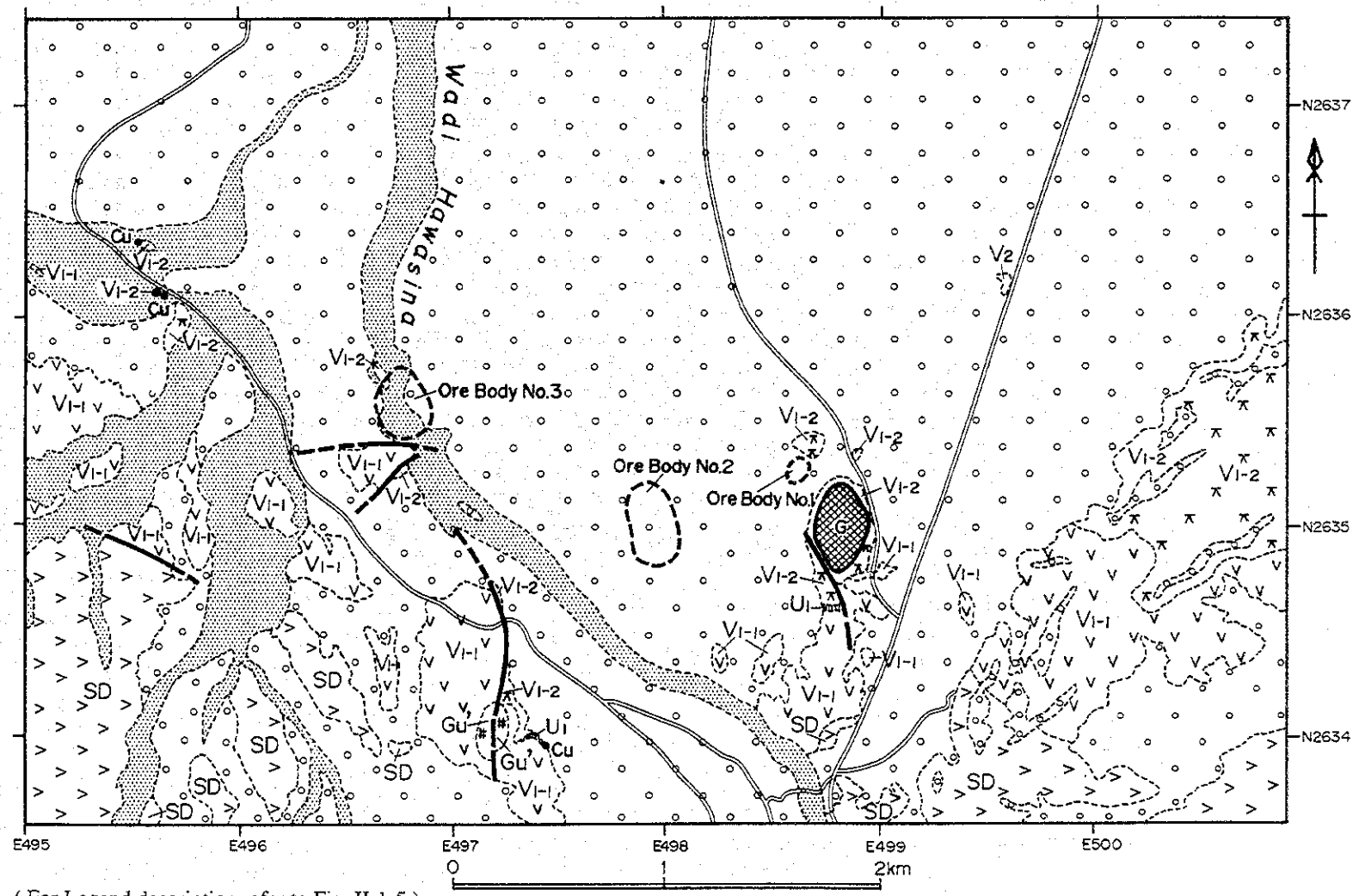

(For Legend description refer to Fig. II-1-5.)

Fig. II -1-2 Geologic map of Ghuzayn area

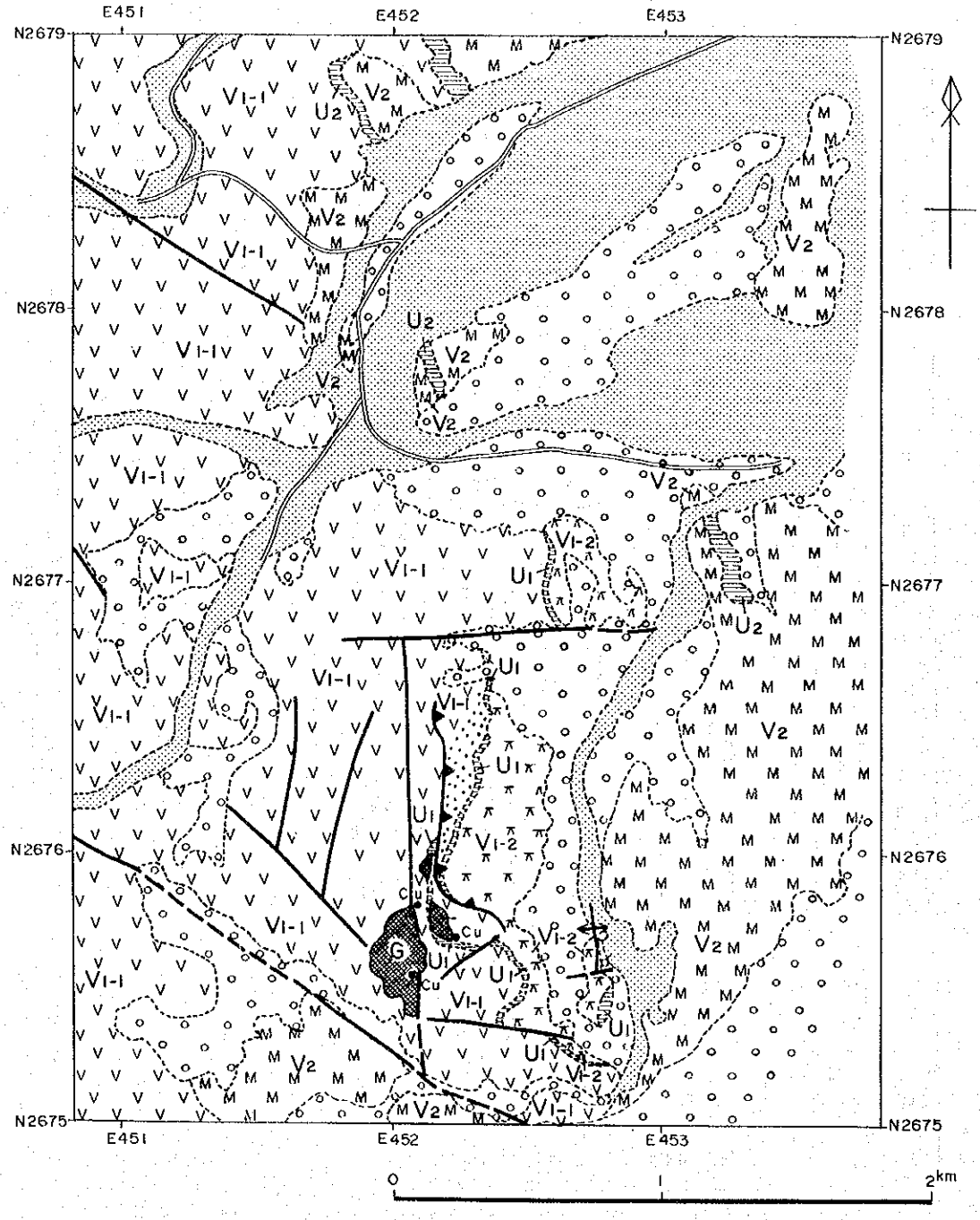

(For Legend description refer to Fig. II-1-5.)

Fig. II-1-3 Geologic map of Zuha area

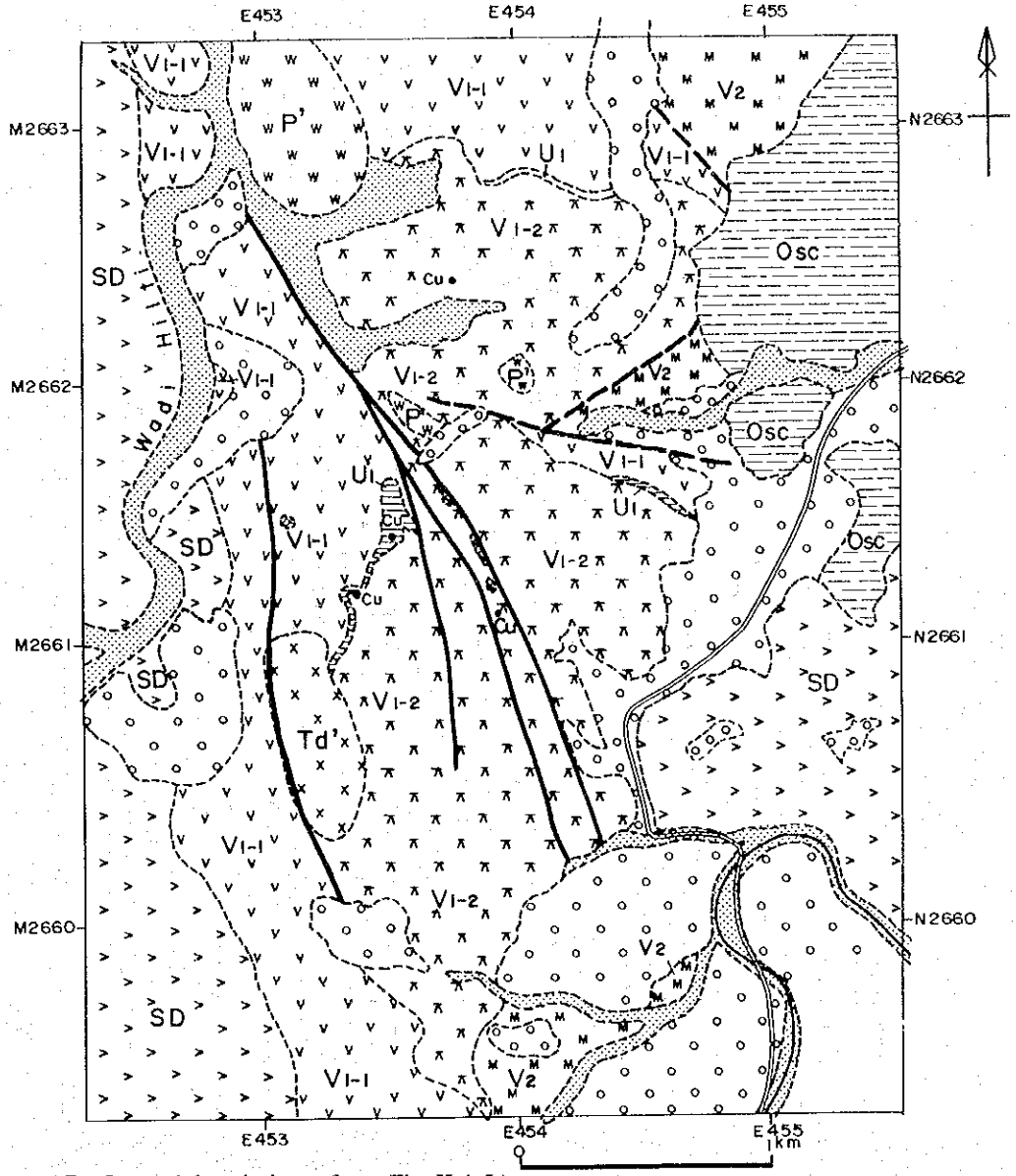

(For Legend description refer to Fig. II-1-5.)

Fig. II-1-4 Geologic map of Maqail area

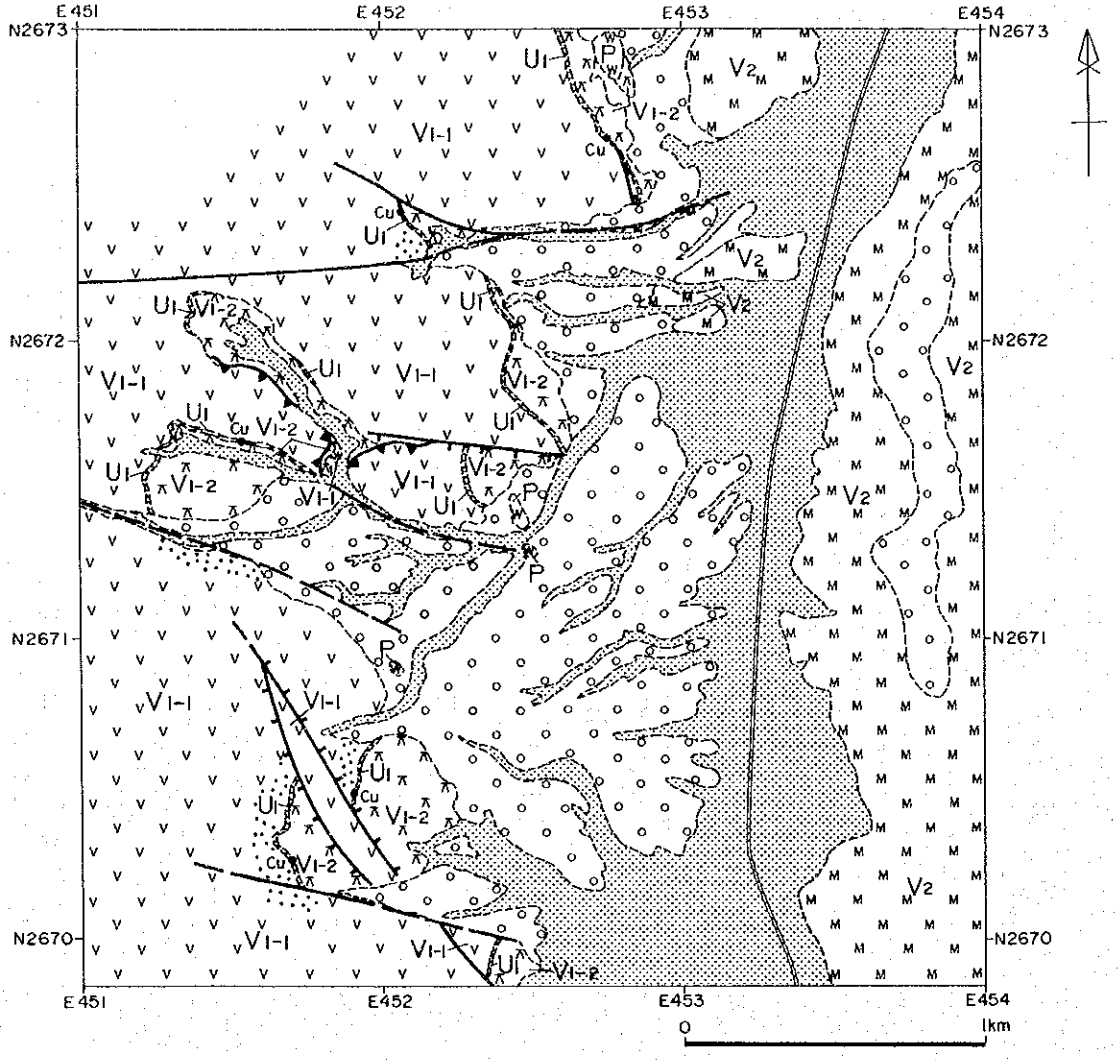

LEGEND

- Wadi sediments
- Alluvial fans and alluvium
- Batinah Olistostrome
  - Osl — Limestone dominant facies
  - Osc — Chert dominant facies
- Middle Volcanic Rocks
  - Middle extrusives
    - V2 — Basaltic pillow lava and massive lava
    - U2 — Metalliferous sediments
  - U1 — Metalliferous sediments
  - Lower Volcanic Rocks
    - Lower extrusives
      - V1-2 — Lower extrusive 2; basaltic pillow lava and massive lava
      - V1-1 — Lower extrusive 1; basaltic pillow lava and massive lava
- Sheeted-dyke Complex
  - SD — Doleritc and basaltic dyke
- Intrusive Rocks
  - Td' — Trondhjemite
  - P' — Peridotite
  - Gu' — Gabbro

ECONOMIC GEOLOGY SYMBOLS

- G — Gossan
- Strongly silicified zone
- Strongly epidotized zone
- Cu — Copper mineralization

STRUCTURAL FEATURES

- Fault; dashed where inferred
- Thrust fault
- Anticline
- Syncline

Fig. II-1-5 Geologic map of Salahi area

V1-2 consists of pillow lava as well as massive lava. Thick massive lava, with 5m in maximum thickness, is found directly over U1. U1 continuously crops out showing a thickness of about 30 to 50cm. The gossan located in the area graded laterally from this U1, which has a bigger thickness than U1 and is intensely brecciated. The area shows a complicated geological structure consisting of thrust fault, normal fault and folding.

The gossan in this area has almost the same scale as the one in Ghuzayn. Copper mineralization can be seen in many places around the gossan. An ancient smelting site was located in the vicinity of the gossan. Intense epidotization is observed in V1-1 at the contact with V1-2 around the gossan.

In this area from 1974 to 1976 Prospection Ltd. carried out drilling, geological, geochemical as well as geophysical surveys. In 1985 Bishimetal Exploration Co., Ltd. conducted geological and geochemical exploration works. Moreover in 1991, DNPM carried out drilling survey. Table II-1-1 indicates a brief description of the results of the drilling works carried previously in Zuha.

1-3-3 Maqail Area

Maqail area is located 40km southwest of Saham City and includes not only inside but also the surroundings of the Maqail south mineral showing which was surveyed during the Phase I.

As indicated in Fig.II-1-4, the geology of this area consists mainly of SD, V1-1, V1-2, U1, V2, bedded chart of Batinah Olistostrome, and Quaternary sediments. U1 is well exposed in this area, reaches about 2m in thickness at the western side of the central part, is well bedded and contains abundant magnetite. Many basalt and dolerite dikes are intruded into V1-2 at the central and southern parts where a NNW-SSE trending fault runs in V1-2.

Since magnetite predominates in U1 and copper mineralization can be observed in many places, it is likely that U1 graded laterally into a massive sulphide ore. Additionally, silicified zone that is exposed along the NNW-SSE trending fault mentioned above is found in places accompanied by copper mineralization.

1-3-4 Salahi Area

Salahi area is located to the south of Zuha area and about 9km north of Maqail area. The geology of Salahi area consists mainly of SD, V1-1, V1-2, U1, V2 of Samail Ophiolite and Quaternary sediments.

Peridotites are intruded around the boundaries between V1-1 and V1-2 in three places. Many E-W trending faults are found and a thrust fault can also be seen. A NW-SE trending fault observed in the south is considered to be formed during the formation of V1-2.

Regarding the mineral showing, U1 with copper oxides and magnetite are found in several places and intense epidotization in places. Bedded U1 observed in the north, includes abundant magnetite with copper oxides, reaches 2m in thickness and presents quite characteristics that resembles the edge of massive sulphide orebody.

Table II-1-1 Summary of previous drilling works in Zuha area

Holes	Coordinate		Executed length	Direction	Inclination	Executer and Year	Description
	N (km)	E (km)	(m)				
59-1	2,675.480	452.120	91.44	N80°W (280°)	-60°	Prospection Ltd. 1976	-8.38m～-10.52m: gossan zone. Pyrite and minor chalcopyrite disseminations. Silicification and chloritization in places. The highest grade is 0.18%Cu(-44.19m～-46.08m).
59-2	2,675.430	452.125	91.44	N80°W (280°)	-60°	Prospection Ltd. 1976	Random specks of pyrite and chalcopyrite. The highest grade is 0.42%Cu(-58.06m～-59.44m).
59-3	2,675.410	451.955	91.44	N80°W (280°)	-60°	Prospection Ltd. 1976	Specks of pyrite in places. Epidote and hematite are observed.
59-4	2,675.435	452.095	45.72	-	-90°	Prospection Ltd. 1976	Specks of pyrite in places. Rod broken, hole was abandoned.
ZU-1	2,675.900	452.350	187.30	S45°W (225°)	-60°	DNPM 1991	Massive sulphide was not detected.
ZU-2	2,675.750	452.450	251.00	S80°W (260°)	-60°	DNPM 1991	Massive sulphide was not detected.

CHAPTER 2 TDIP SURVEY

2-1 Background and Objectives

TDIP survey was carried out during this phase in order to extract mineralized zones related to the existence of massive sulphide deposits in the South Batinah Coast area on the basis of the results of the geological survey previously carried out.

This fiscal year corresponds to the third year since this project started. During the previous cooperative Mineral Exploration project carried out from 1995 to 1996, massive sulphide ore bodies were discovered in Ghuzayn area.

Due to the possibility of discovering additional deposits in Ghuzayn area, more TDIP geophysical survey was carried out to the east and west of the already surveyed area in 1997.

In Maqail area, it was decided to extend the investigation to the north of the previous survey conducted last year. Again and on the basis of the geological indicators extracted during 1997, it was decided to clarify in more detail by TDIP survey whether or not the surrounding of the mineralized zones in Zuha and Salahi areas give promising results.

2-2 Survey Locations and Specifications

During this fiscal year, the following 5 areas were selected for exploration work: Ghuzayn (East and West), Zuha, Maqail and Salahi. A summary of the TDIP survey performed in the above mentioned 5 areas is indicated in Table II-2-1.

2-3 TDIP Survey Method

2-3-1 Procedure

The TDIP survey was carried out by using a time-domain method and adopting a dipole-dipole electrode configuration with a separation factor from 1 to 4. IP data were taken along lines every 100m by keeping a potential dipole of 100m. In the survey area, the TDIP survey is carried out by injecting a current into the earth through current electrodes and the resulting voltage is measured across potential electrodes. Fig.II-2-1 shows the array utilized as well as the location of the plotting points.

For TDIP surveys, the current is turned on for a certain length of time (on-time) then turned off (off-time). The transmitted waveform is then repeated with current flow in opposite direction. The pair of positive and negative on-off waveforms constitutes a cycle, which in this survey lasted 8 seconds, as indicated in Fig.II-2-2. According to Fig.II-2-3, the polarization of the target creates a transient decay voltage and its corresponding changing response is observed in the received waveform.

Table II-2-1 Survey amounts of TDIP

AREA	Length(km)	Number of Lines	Number of Points
Ghuzayn(EAST)	12.4	0.4 km× 6 Lines 2.0 km× 5 Lines	426
Ghuzayn(WEST)	17.8	2.1 km× 4 Lines 2.3 km× 2 Lines 2.4 km× 2 Lines	600
Maqail	12.0	1.7 km× 1 Lines 2.0 km× 2 Lines 2.1 km× 3 Lines	396
Zuha	34.5	2.0 km×13 Lines 2.5 km× 1 Lines 3.0 km× 2 Lines	1156
Salahi	21.6	1.0 km× 5 Lines 1.5 km× 7 Lines 1.7 km× 1 Lines 2.2 km× 2 Lines	654
Total	98.3	56	3232

2-3-2 Instrumentation

The instrumentation used for the conventional time-domain IP survey is described in the Table II-2-2.

Table II-2-2 Specifications of TDIP survey instruments

Receiver	**Zonge GDP-16**	**Phoenix V5**
Frequency range	DC to 8KHz	DC to 10KHz
Number of Channels	3	8
Number of Stackings	8096	No restriction
Detectable signal	1 μ V	1 μ V
A/D Conversion	16 bits	16bits
Number of Windows	13(from 50 to 1930ms)	13(from 50 to 1550ms)
Transmitter	**CH-95A**	**IPT-1**
Output Power	2kw,800v,12A	2kw,800v,10A
Output Frequency	DC to 10KHz	DC to 12KHz
Frequency control	Automatic	Automatic
Generator	**Geonics GPU2000**	**Robin**
Maximum output	2Kw	3Kw
Output Voltage	200V	200V
Output Frequency	400Hz	50Hz

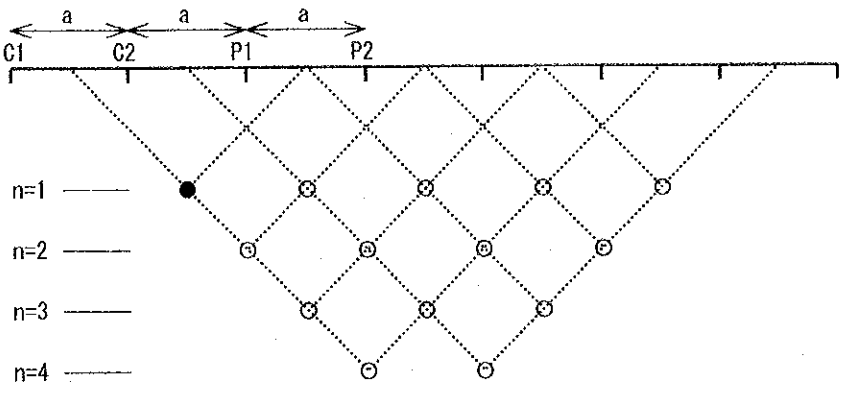

Fig. II -2-1 Dipole-dipole array and plotting procedure

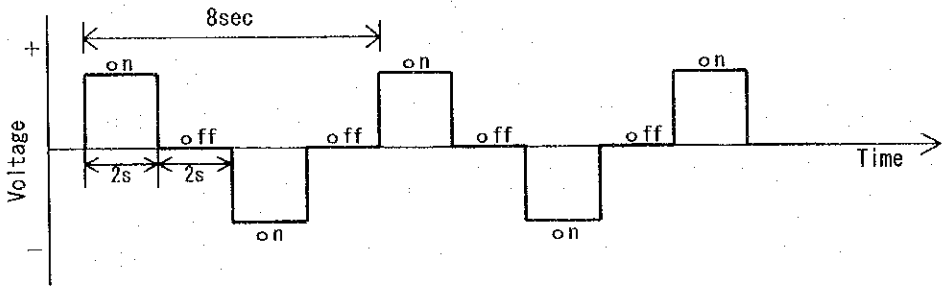

Fig. II -2-2 Waveform produced by the transmitter

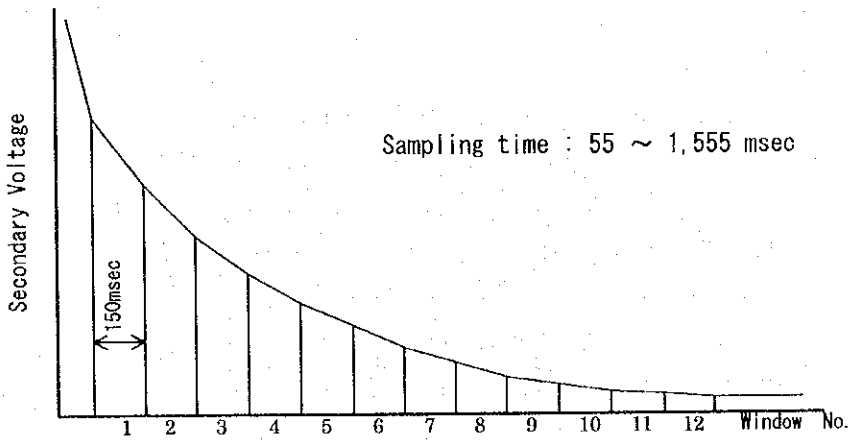

Fig. II -2-3 Sampling interval of the TDIP receiver

2-4 Analysis Method

2-4-1 Data processing

The TDIP data processing involves the determination of 3 parameters, i.e., apparent resistivity, chargeability as well as metal factor. The first 2 parameters are calculated directly by the receiver unit during data acquisition. The third one is calculated as a simple relation between the first 2 parameters. These 3 parameters are calculated as follow:

a) Apparent resistivity (ρ)

$$\rho = K\frac{V_p}{I}$$

Where, $K = \pi an(n+1)(n+2)$ and Vp is the received voltage in volts, a is the A-spacing in meters, n is the N-spacing and I is the transmitted current in Amperes.

b) Chargeability (M)

$$M = \frac{1}{V_p}\int_{t_1}^{t_2} V_t dt$$

Where, Vp is the primary voltage in volts and Vs is the secondary voltage in volts.
Here, the secondary voltage is calculated from 55msec. to 1555msec.

c) Metal factor (MF)

$$MF = \frac{M}{\rho}\times 100$$

Where, M is the chargeability (mV/V) and ρ the apparent resistivity (Ω-m)

2-4-2 Topographic corrections

Since the apparent resistivity is calculated here as a function of the location of the current and potential electrodes on a half-infinite plane, it is affected by topography depending on the location of the electrodes. For the case of a dipole-dipole configuration, the apparent resistivity appears to be high beneath a hill and low beneath a valley. On the other hand, the chargeability values are less affected by topography.

In order to make the appropriate corrections for the present survey, a 2D analysis that takes into account the topographical elevation of the surveyed points was applied to each line of the survey. The corrected apparent resistivity values are then used to construct the related sections and contour maps.

2-4-3 Two-dimensional analysis

For the TDIP data analysis and according to the standard model, the apparent resistivity and chargeability distributions are used in combination to make a quantitative analysis of the pseudo-sections

and plan maps. The resultant underground model is inferred by making use of the theoretical results given by the model.

In the present survey, according to the limitations of the results of the forward modeling and to match the field results, it was used a 2D inversion model which combines the FEM forward calculations with a non-linear least square method. The inconveniences presented by the 1D analysis to make a layer analysis of the underground structure are best solved by the approximation made by the 2D model.

In order to make the model calculations, the underground structure is divided into many small blocks, each of them having initially assigned their own chargeability and resistivity value. The blocks are designed so that small blocks are placed close to the surface and increased in size as the blocks are located at deeper levels.

2-5 Survey Results

2-5-1 Electrical measurements of rock samples

Representative rock samples from the survey area were analyzed in order to investigate whether the contrast in resistivity between the target mineralization and the volcanic rocks is enough to discriminate between these units in terms of electrical properties.

In general, resistivity and IP measurements in rocks may not reflect in a direct way the intrinsic resistivity or chargeability because of different degree of alteration and water content over the survey area, however clear ideas can be obtained related to the relative variations between rocks units and mineralization.

(1) Measurement method

Measurement of the electrical properties of rock samples, such as resistivity and IP chargeability were carried out on some samples selected from the survey area. The rock samples were formed into a cylindrical shape and thereafter, soaked into water for a reasonable amount of days but not less than 48 hours. Apparent resistivities as well as chargeability values were measured according to the IP time domain procedures in the laboratory. For this purpose, it was used a Lab Downhole Transmitter LDT-10 made by Zonge. During the determinations of the resistivity and chargeability values, the following formulas were utilized:

For Resistivity:

$$\rho = \frac{A}{L} \times \frac{V_p}{I}$$

where ρ is resistivity (ohm-m), A is the section of the sample (m^2), L length of the rock sample (m), Vp the voltage (V) and I the current (A)

For Chargeability:

$$M = \frac{1.87}{V_p} \times \int_{t1}^{t2} V_s dT$$

where M is the chargeability(mV/V), Vp the primary voltage (V), Vs the secondary voltage (mV), dT

the sampling interval (sec), *t1* the off-time voltage 500msec and *t2* the off-time voltage 1,100msec

(2) Results

Results of the electrical properties of rocks samples measured in the laboratory are indicated in Table II-2-3.

The resistivity values measured in the laboratory ranged from 22 to 34,600 Ω-m.

Resistivity measurements in pillow lava and massive lava samples indicated values in the range between 100 to 500 Ω-m. However, the test on the sample No. 10 of pillow lava in V1-1 indicated a resistivity of about 42 Ω-m in contrast with the samples Nos. 13 and 20 of pillow lava in V1-2 that showed high resistivity values (1535 Ω-ohm and 822 Ω-ohm-m, respectively). According to these results, the values in resistivities between V1-1 and V1-2 did not show any remarkable difference.

The laboratory tests in dyke rocks samples Nos.3, 4 and 7 of dolerites ranged between 200 to 600 Ω-m and the sample No.16 of basalt indicated high resistivity values around 1000 Ω-m. The intrusive rocks samples Nos.21 to 23 of peridotite indicated high resistivity values that ranged between several thousands of Ω-m, in contrast with the resistivity values obtained for the sample No.24 of gabbro that showed a low resistivity of about 22 Ω-m.

Regarding the chargeability measurements, the values measured in the laboratory ranged between 0.1 to 44mV/V. Disseminations of pyrite indicated in general high chargeability values. Especially, the sample No.28, which is pillow lava intensely disseminated, indicated high chargeability values of 44mV/V. The samples Nos.8 to 10 and 12 which are pyrite disseminations were confirmed with chargeability values as low as 4mV/V. The samples Nos.13 and 20, which indicated high resistivity values, did not show pyrite disseminations, but high chargeability values of about 30mV/V were measured. All of the intrusive rocks indicated low chargeability values of less than 3 mV/V.

2-5-2 Ghuzayn area

(1) Lines location

A total of 14 lines were surveyed around the east side as well as the west side of Ghuzayn area.

In the east side, a total of 6 lines (400E to 1400E) were extended 400m each towards the north and new 5 lines (1600E to 2400E) of 2.0km each were located on the east side.

In the west side, a total of 8 lines were set up as follows: 4 lines (600W to 1200W) of 2.1km each, 2 lines(1400W and 1600W) of 2.3km each and 2 lines(1800W and 2000W)of 2.4km each. The direction of the lines are N40° E in the east side and N20° E in the west side. These directions are same as the 1995 field survey season.

Fig. II -2-4 shows the location of all the IP lines surveyed between 1995 and 1999.

(2) Results

Pseudo sections of apparent resistivity, chargeability and metal factor values are presented from Fig. II

Table Ⅱ-2-3 Resistivity and chargeability of rock samples

Sample No.	Borehole and Depth	Resistivity (Ω.m)	Chargeability (mV/V)	Rock Name and Formation	Alteration and Mineralization
1	Z1-22.3m	508	3	Ma(V1-2)	
2	Z1-31.3m	245	18	Ma(V1-1)	Sili, Epi vein, Py vein & diss(sl)
3	Z1-50.0m	180	14	Do(dyke)	Py vein & diss(sl)
4	Z1-70.1m	373	10	Do(dyke)	
5	Z1-85.0m	147	13	Ma(V1-1)	Py diss(sl)
6	Z1-113.4m	314	15	Pw(V1-1)	Sili, Epi diss, Py diss(sl)
7	Z1-141.1m	589	7	Do(dyke)	
8	Z1-166.5m	149	3	Pw(V1-1)	Sili, Qz vein, Py vein & diss(sl)
9	Z1-171.6m	194	3	Ma(V1-2)	Sili, Qz vein, Py vein & diss(sl)
10	Z1-209.5m	42	2	Pw(V1-1)	Sili, Qz vein, Py vein & diss
11	Z1-222.9m	116	14	Pw(V1-1)	Sili, Py vein & diss
12	Z1-238.8m	187	4	Pw(V1-1)	Sili, Qz vein, Py vein & diss
13	M1-30.9m	1,535	26	Pw(V1-2)	Sili
14	M1-61.6m	484	9	Ma(V1-2)	Sili, Py diss(sl)
15	M1-91.0m	356	8	Pw(V1-2)	Sili, Ca, Py diss(sl)
16	M1-135.3m	936	9	Ba(dyke)	
17	M1-155.7m	166	26	Pw(V1-2)	Sili, Py vein & diss
18	M1-192.8m	218	14	Pw(V1-2)	Sili, Py vein & diss(sl)
19	M1-225.8m	561	13	Pw(V1-2)	Sili, Qz vein, Py vein & diss(sl)
20	M1-268.0m	822	29	Pw(V1-2)	Sili
21	M2-31.4m	3,299	1	Pe	
22	M2-59.4m	34,600	2	Pe	
23	M2-115.8m	28,860	2	Pe	
24	M2-138.3m	22	3	Gb	
25	M2-144.4m	122	3	Ma(V1-1)	
26	M2-165.7m	1,733	0.1	Pw(V1-1)	Sili, Epi diss
27	M2-190.3m	496	4	Pw(V1-1)	Sili, Epi vein & diss, Py-diss
28	M3-132.2m	289	44	Pw(V1-1)	Sili, Qz vein, Py vein & diss(in)
29	M3-143.3m	417	6	Pw(V1-1)	Sili, Epi vein
30	M3-147.1m	431	6	Pw(V1-1)	Sili, Epi vein & diss

Remarks

Z: Zuha
M: Maqail

V1-1: Lower Extrusives 1
V1-2: Lower Extrusives 2

Ba: Basalt
Pw: Pillow lava
Ma: Massive lava
Do: Dolerite
Pe: Peridotite
Gb: Gabbro

Py: Pyrite
Ca: Calcite
Epi: Epidots
Qz: Quartz
Sili: Silicified
diss dissemination
vein veinlets
(sl): Slight
(in): Intense

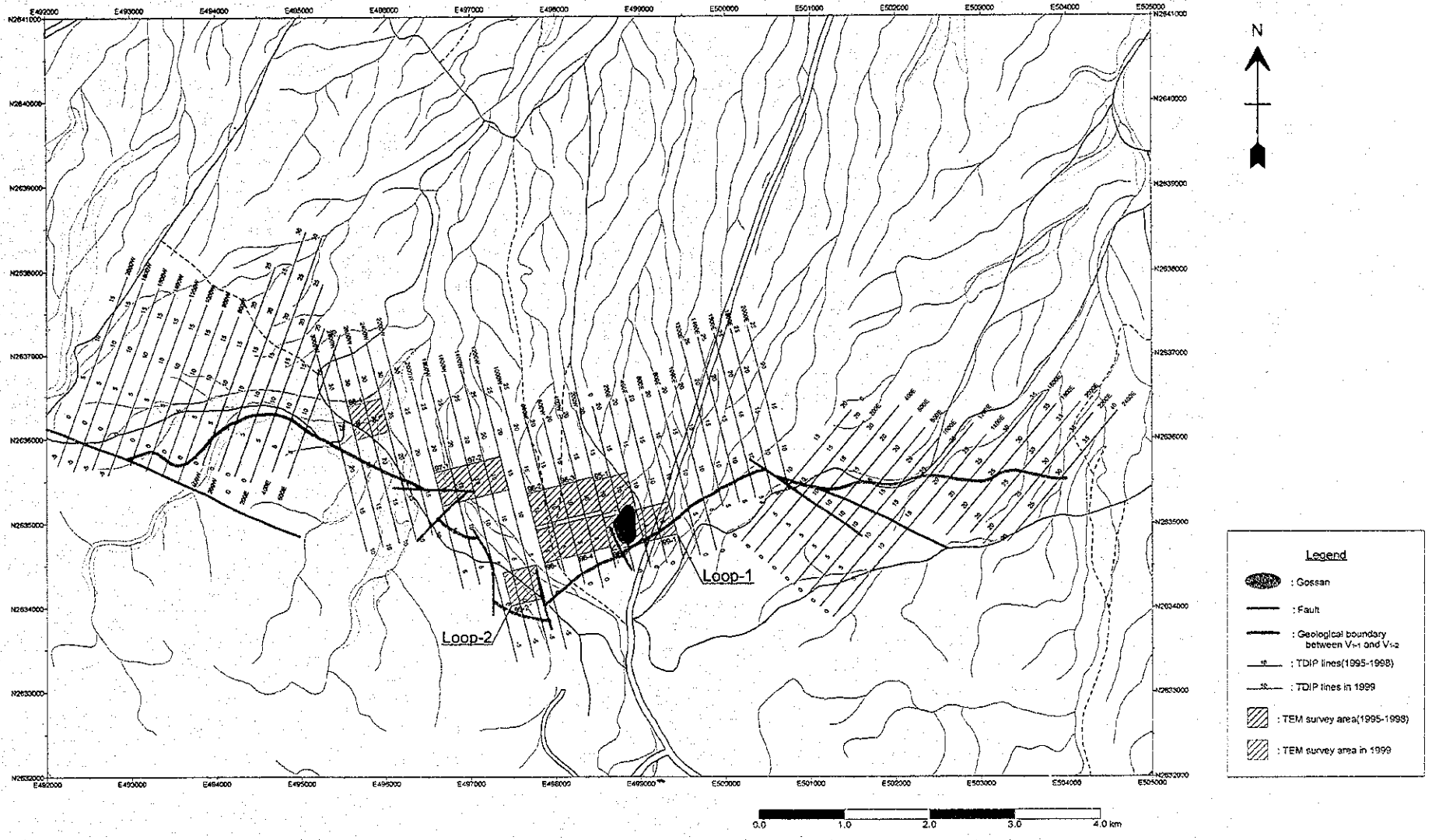

Fig. II -2-4 Geophysical survey location in Ghuzayn area

-2-5(1) to Fig. II -2-7(2) and from Fig. II -2-12 to Fig. II -2-14. Compiled contour maps of apparent resistivity, chargeability and metal factor for n=1 to 4 are presented from Fig. II -2-8 to Fig. II -2-11 and from Fig. II -2-15 to Fig. II -2-18.

According to the apparent resistivity results in the lines 1600E to 2400E obtained during this year in East Ghuzayn, an apparent resistivity structure of trend EW can be seen. Medium to high resistivities were detected in the south side and low resistivities towards the north, being these two structures corresponding geologically to the V1-1 and V1-2 formations respectively (Figs. II-2-8 to II-2-11).

The chargeability distribution shows approximately the same distribution pattern as the apparent resistivity, i.e., medium to high chargeability values in the south and low values in the north. As a result, the metal factor shows entirely low values, clarifying that no clear anomaly leading to the existence of massive sulphide can be expected in this area.

In relation to the Ghuzayn west side (lines 600W to 2000W), the south side shows in general relatively high apparent resistivity values and low in the north side. Moreover, apparent resistivity distribution below 25Ω-m with a tendency to extend to the south (Fig.II-2-15) is seen distributed from the lines 600W to 1400W at deep levels around the station No. 15. Chargeability values are in general low, and in places where low resistivity was detected; metal factor values were also comparatively high. Since the chargeability values were rather low for these cases, it can be stated that these anomalies do not bear any relation to mineralization.

(3) 2D analysis

2D analysis was performed for all the lines, but here for matter of convenience, only the sections containing representative anomalies will be described. On these regards, only the 2D results of lines 1600E and 800W will be briefly described (Fig. II -2-19).

Firstly, in relation to the line 1600E in the east side, it clearly presents a different structure between the north side and the south side from station No.21. In the north side, the apparent resistivity, and the chargeability present low values, but in the south side, the apparent resistivity values are high and chargeability values present moderate values. According to the results in this representative line, there is no evidence to support the existence of massive sulphide.

In relation to the line 800W located in the west side, low resistivity zone is observed at depth of station No.7. Since the chargeability values are about 10mV/V, no massive sulphide can be expected below this section.

2-5-3 Zuha area

(1) Lines location

During this fiscal year, a total of 16 lines were surveyed along N90° E direction with a line spacing of 200m, as follow: 13 lines(0N to 400N and 1200N to 3000N) of 2.0km each, 1 line(1000N) of 2.5km and 2 lines(600N and 800N) of 3.0km each. Fig. II -2-20 shows the location of all the IP lines surveyed in Zuha.

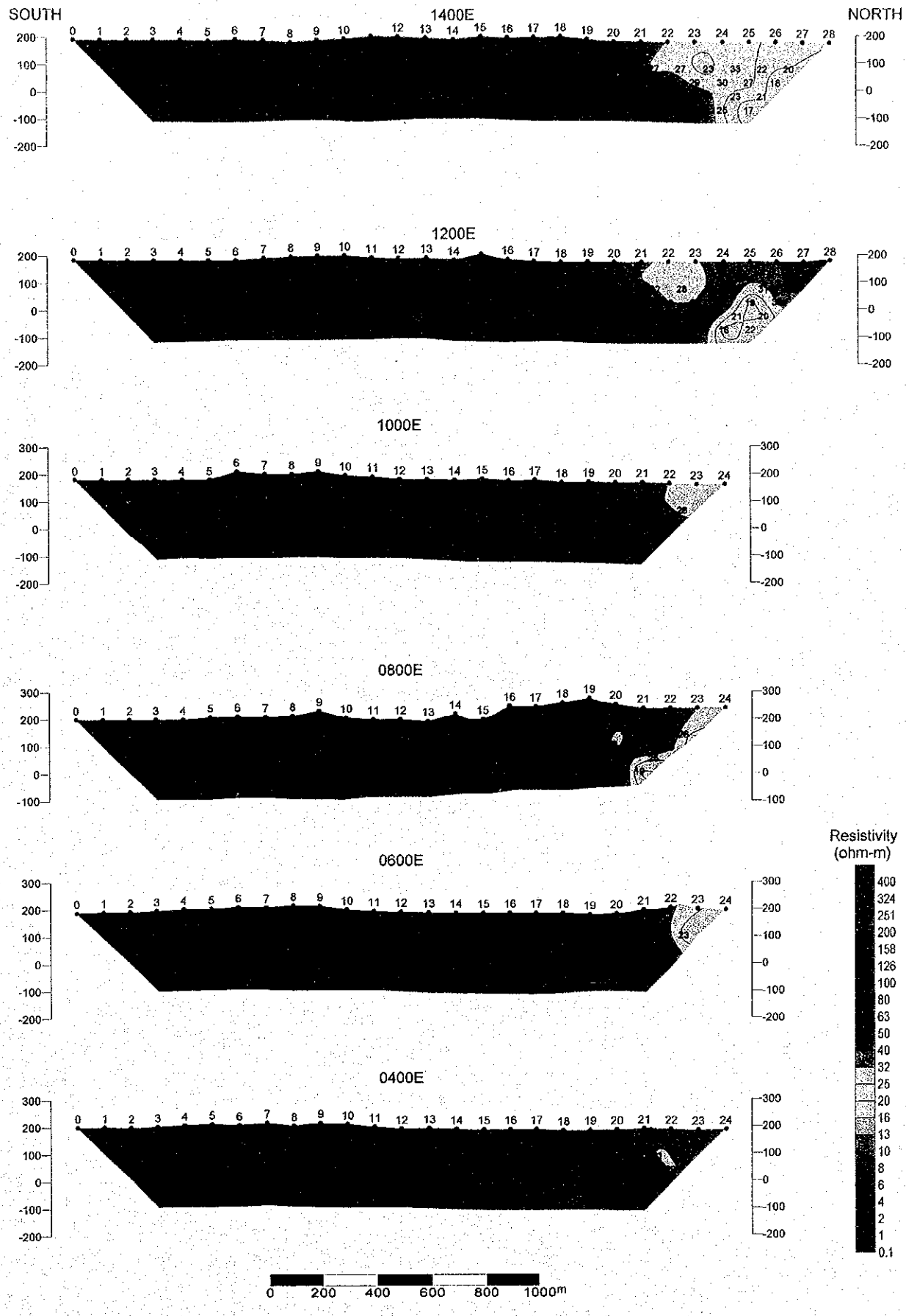

Fig. II-2-5(1) Apparent resistivity pseudo-sections in Ghuzayn area(East)

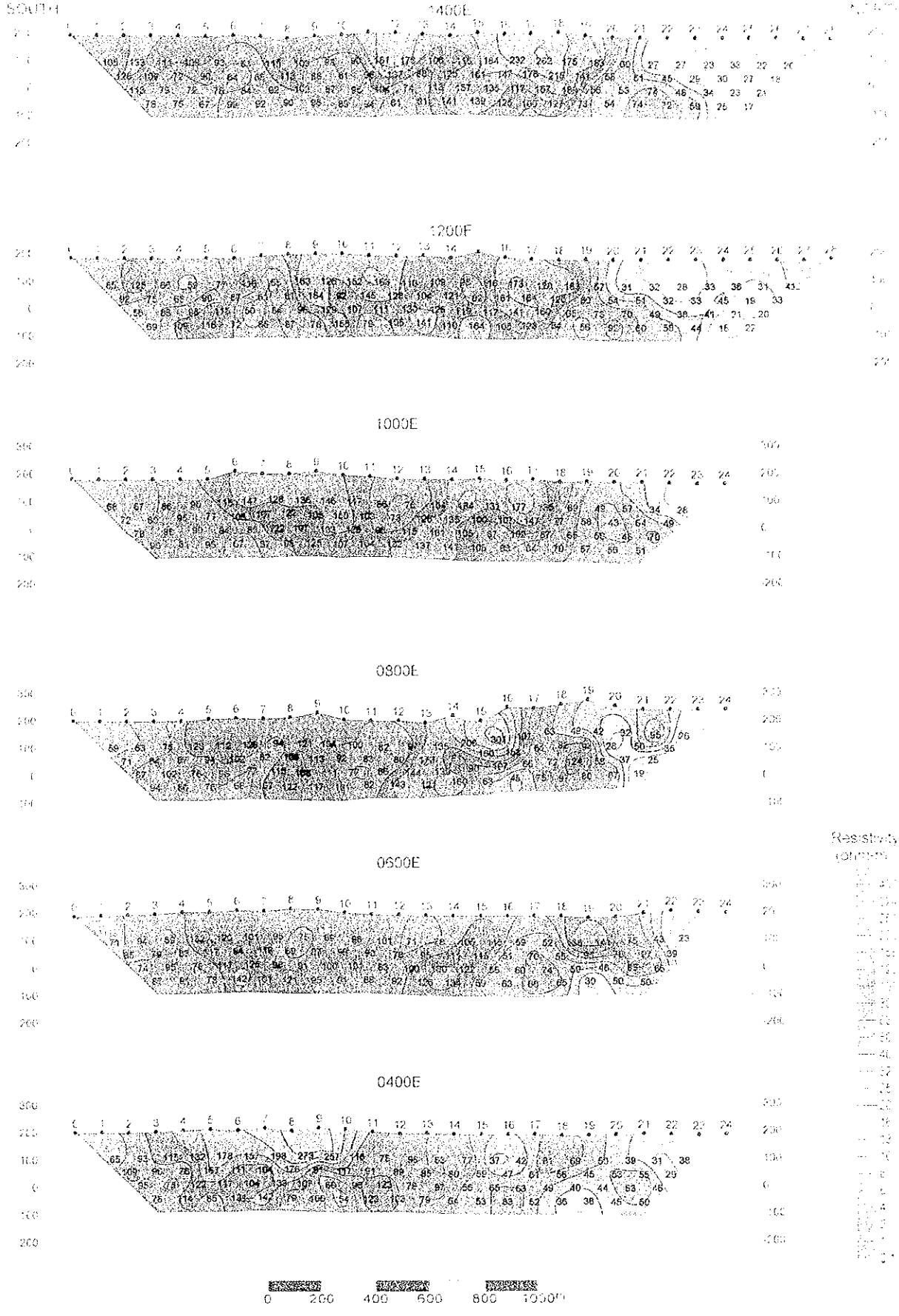

Fig. II-2-5(1) Apparent resistivity pseudo-sections in Ghuzayn area(East)

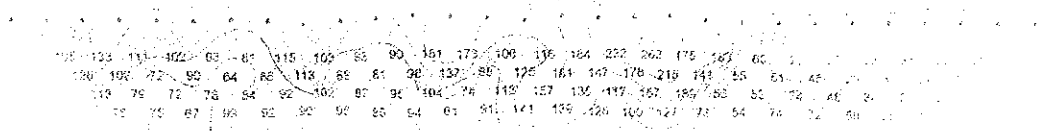

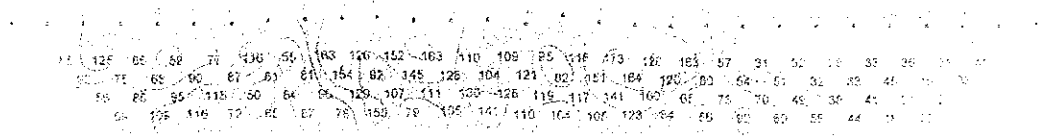

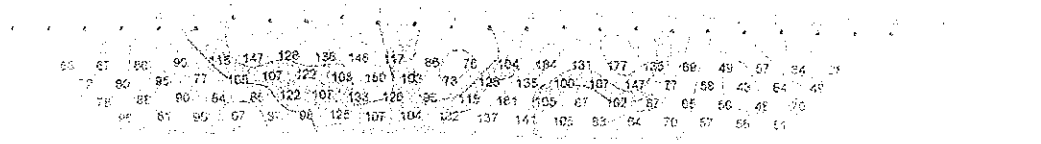

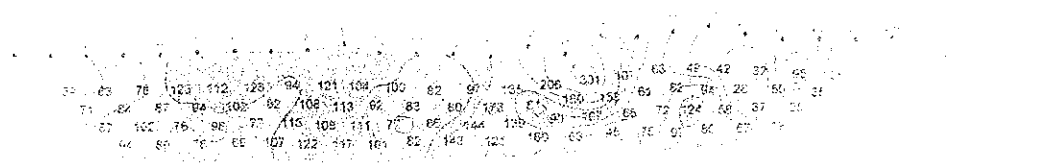

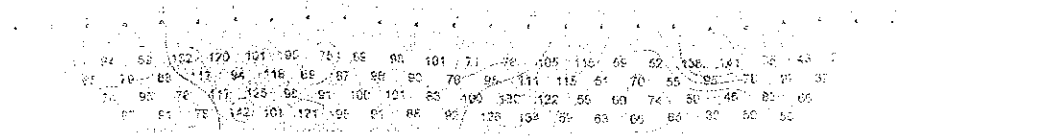

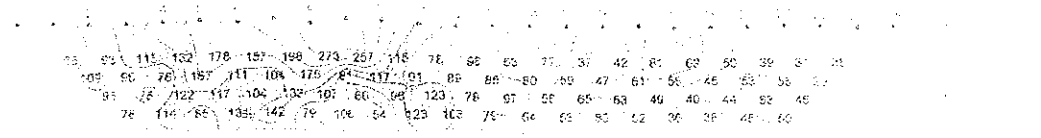

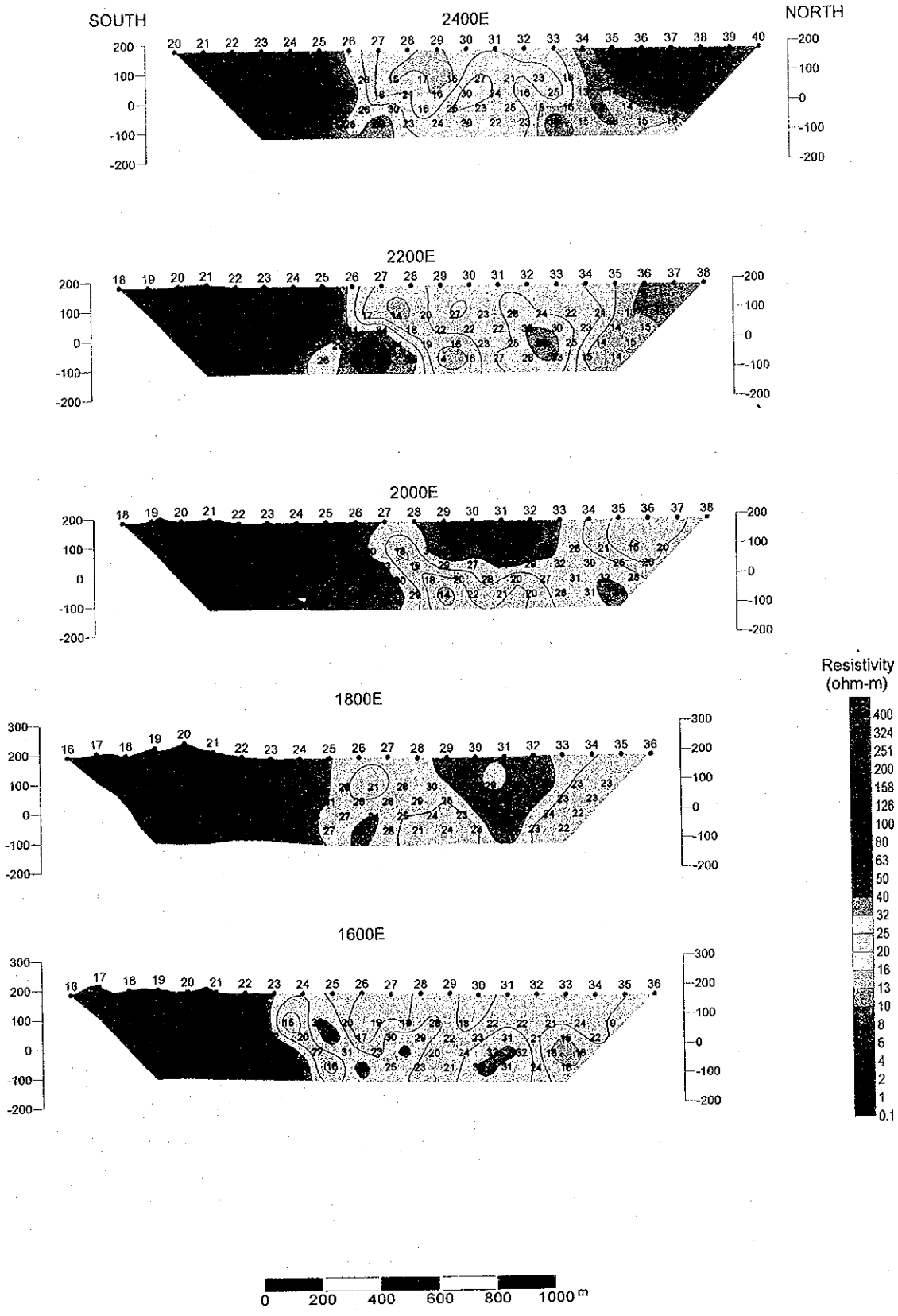

Fig. II -2-5(2) Apparent resistivity pseudo-sections in Ghuzayn area(East)

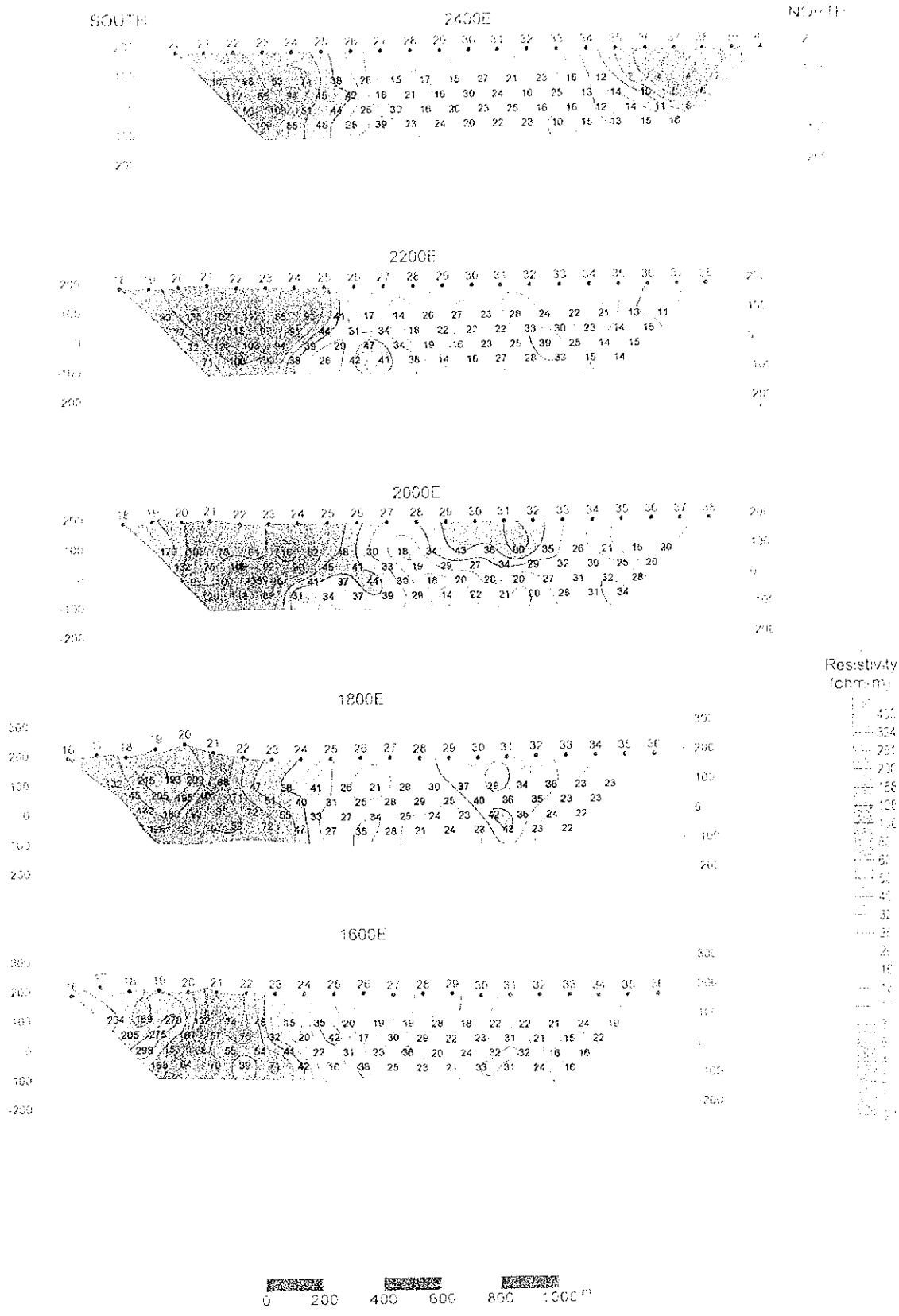

Fig. II -2-5(2) Apparent resistivity pseudo-sections in Ghazayn area(East)

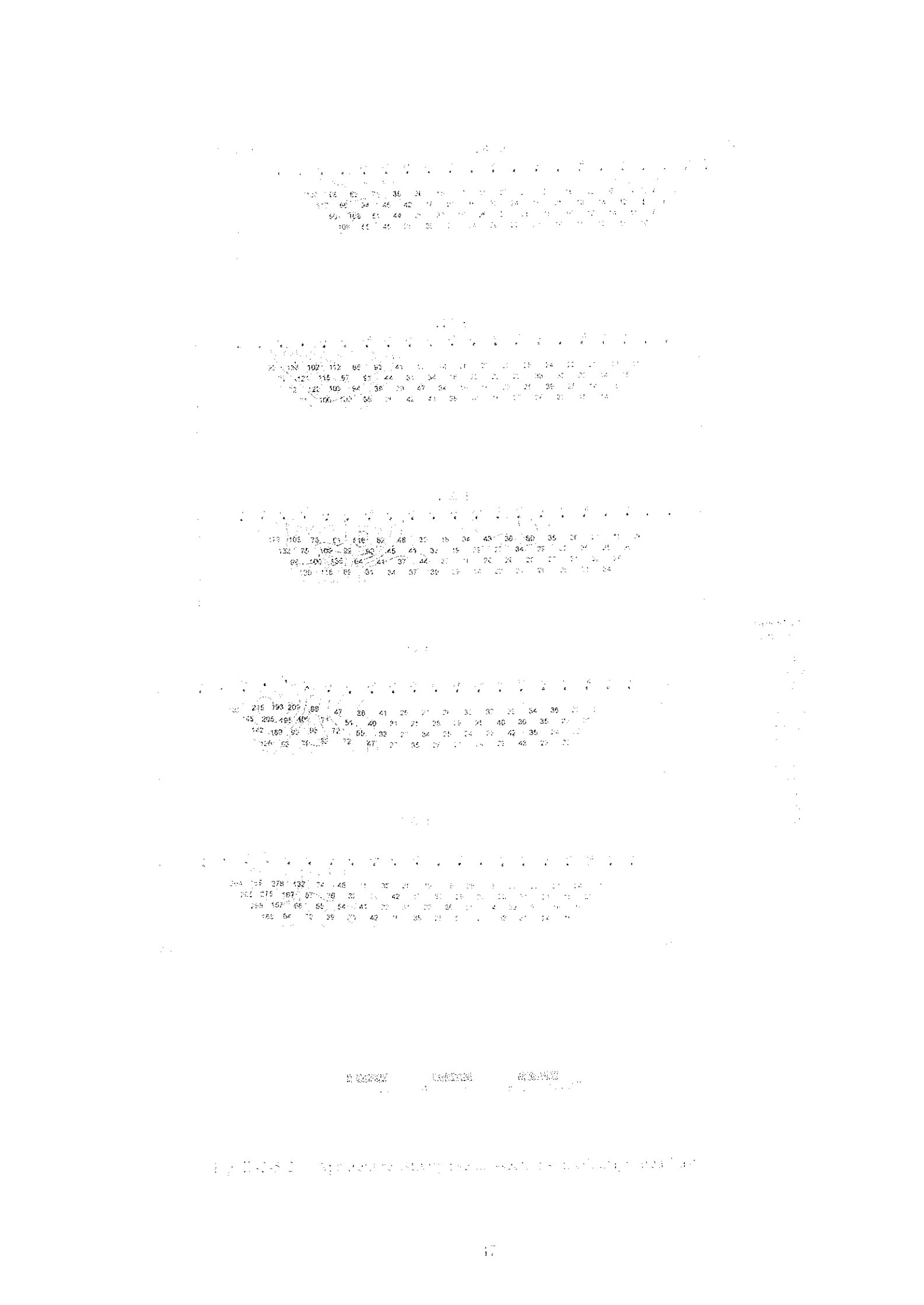

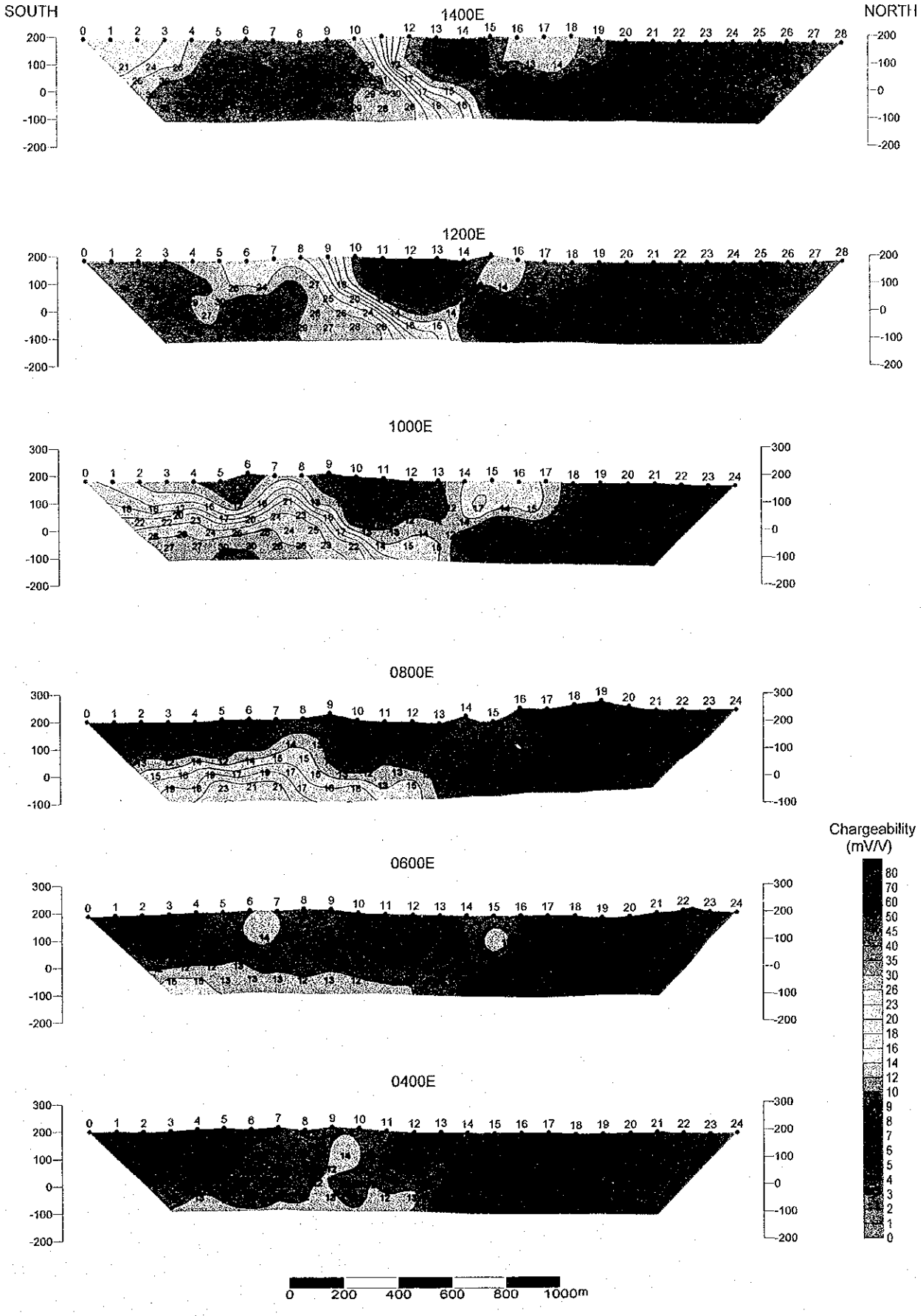

Fig. II -2-6(1) Chargeability pseudo-sections in Ghuzayn area(East)

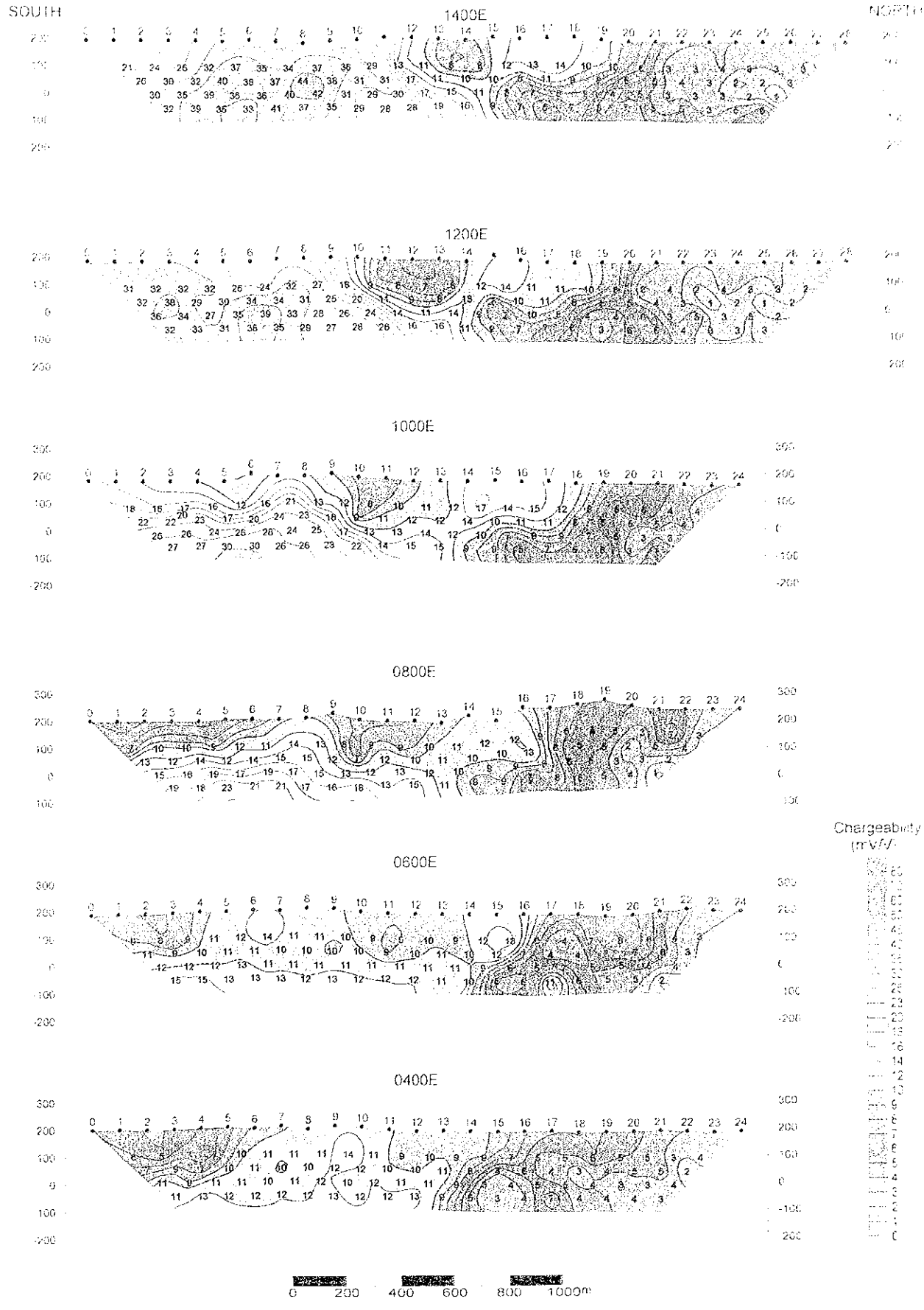

Fig. II-2-6(1) Chargeability pseudo-sections in Ghuzayn area(East)

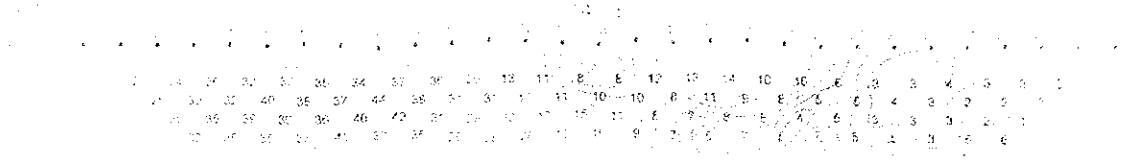

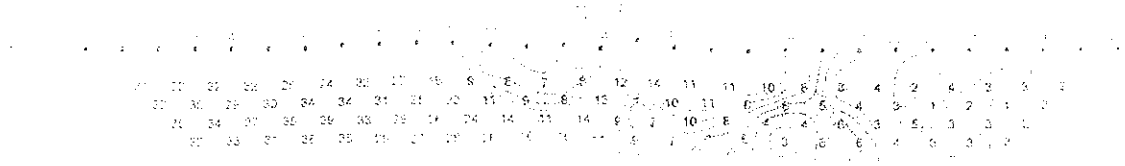

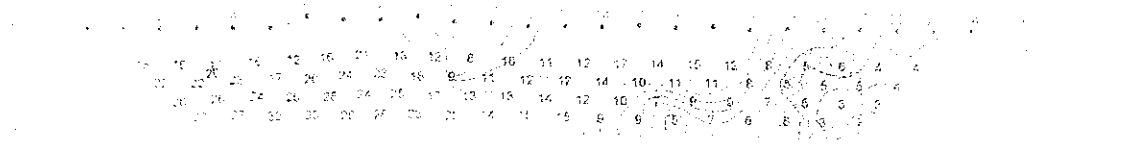

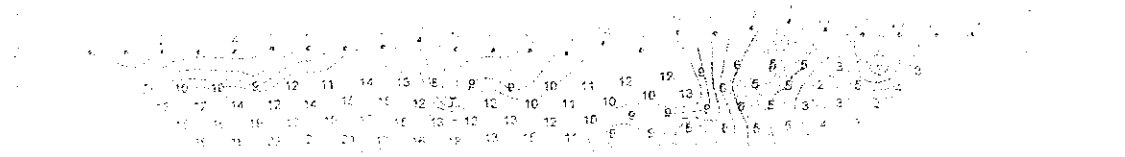

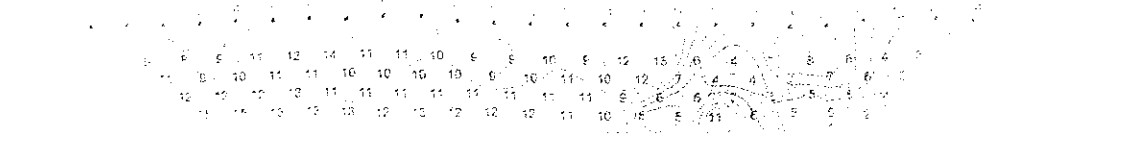

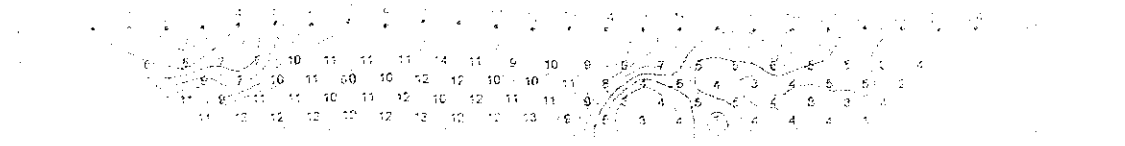

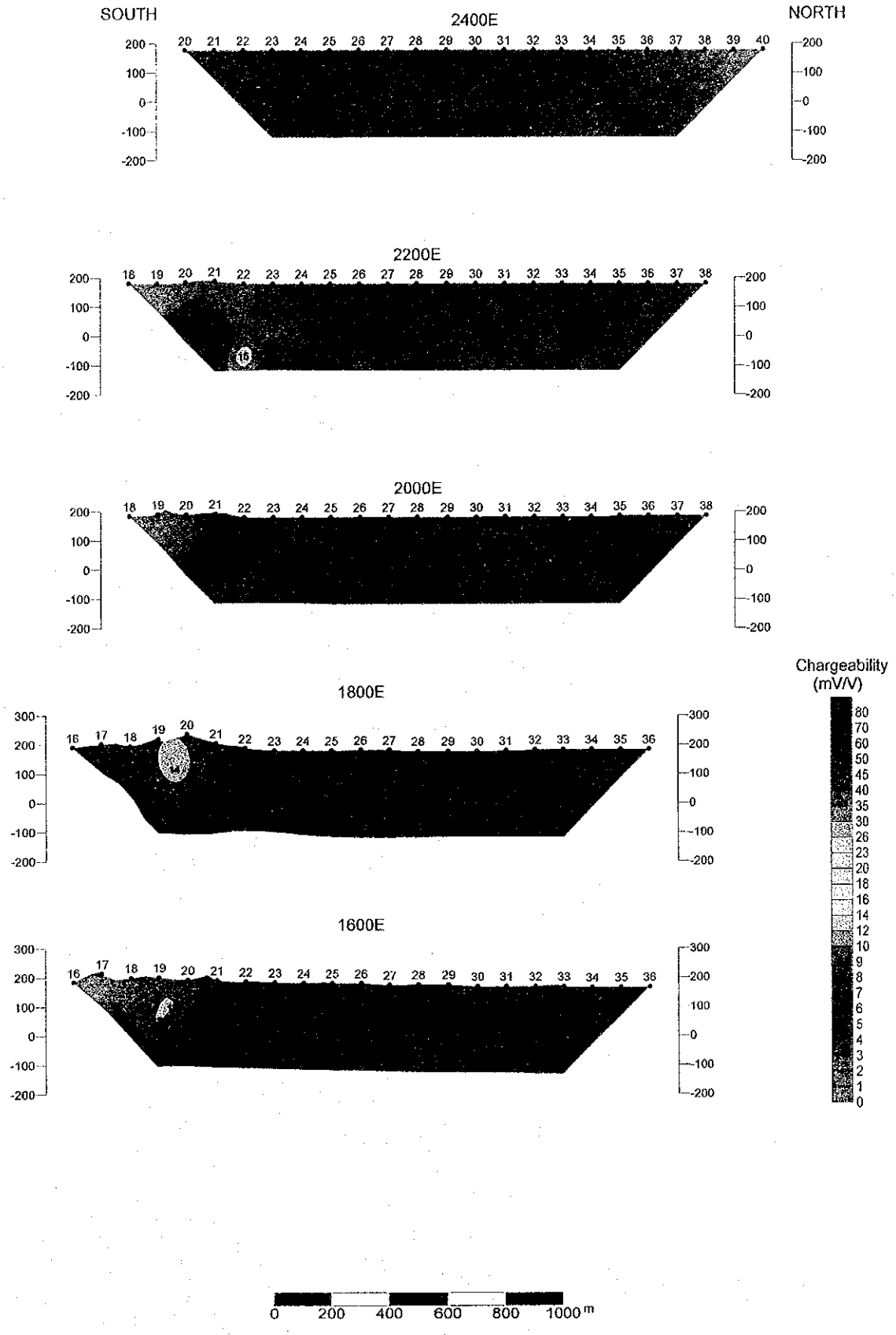

Fig. II -2-6(2) Chargeability pseudo-sections in Ghuzayn area(East)

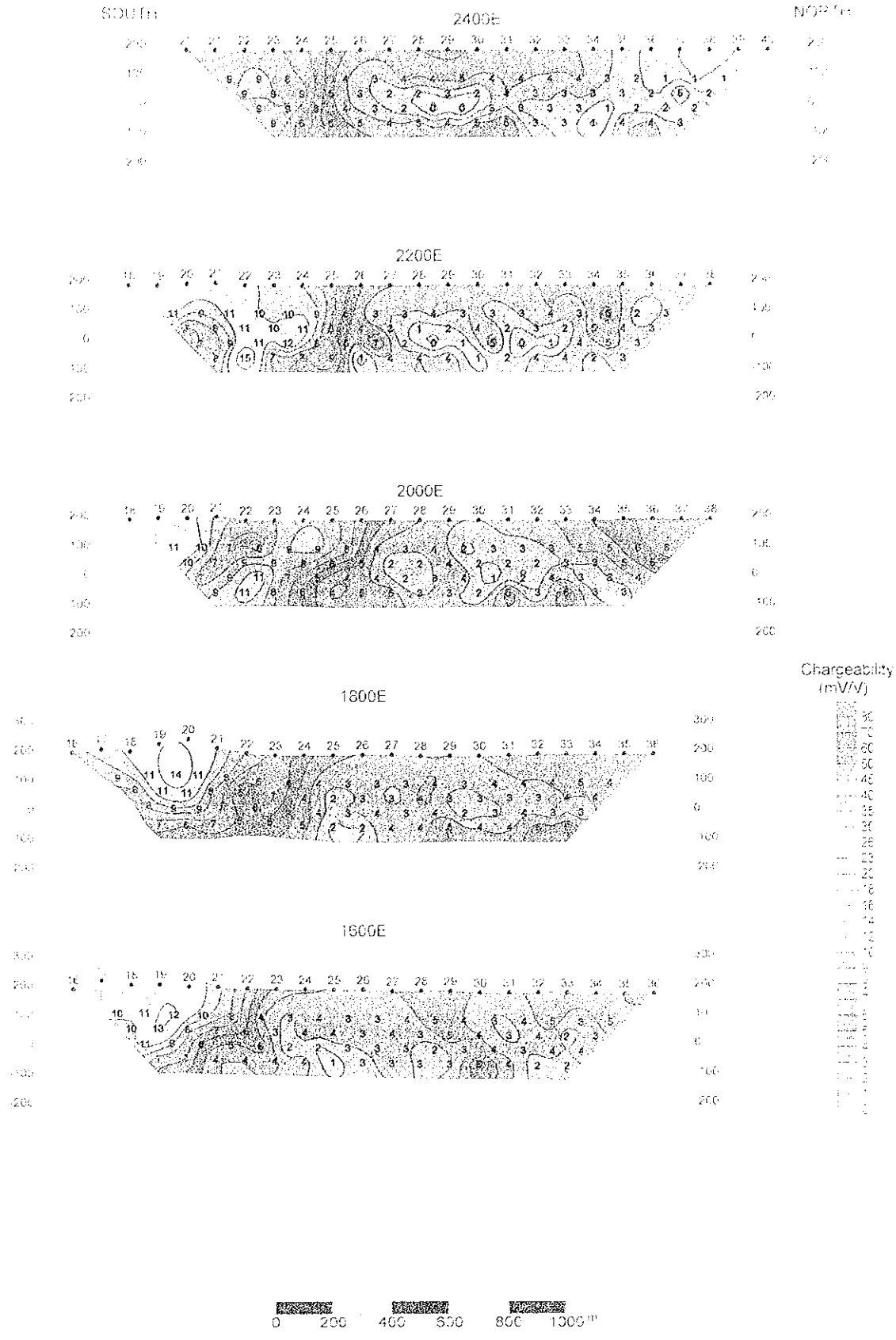

Fig. II-2-6(2) Chargeability pseudo-sections in Ghuzayn area(East)

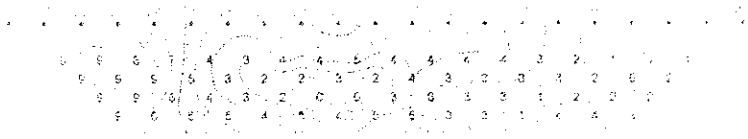

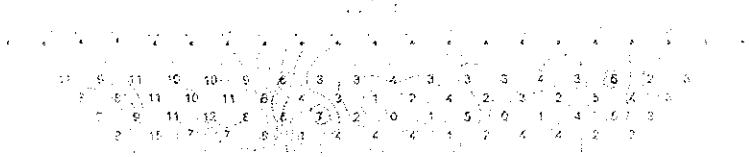

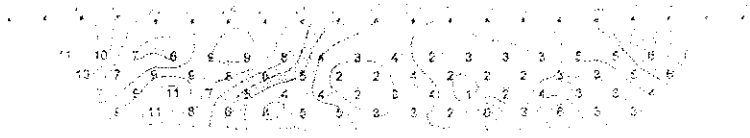

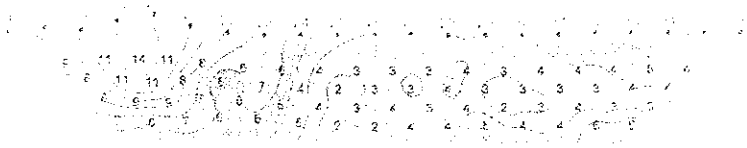

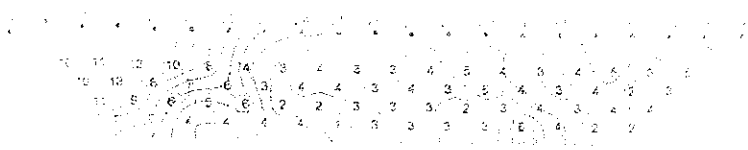

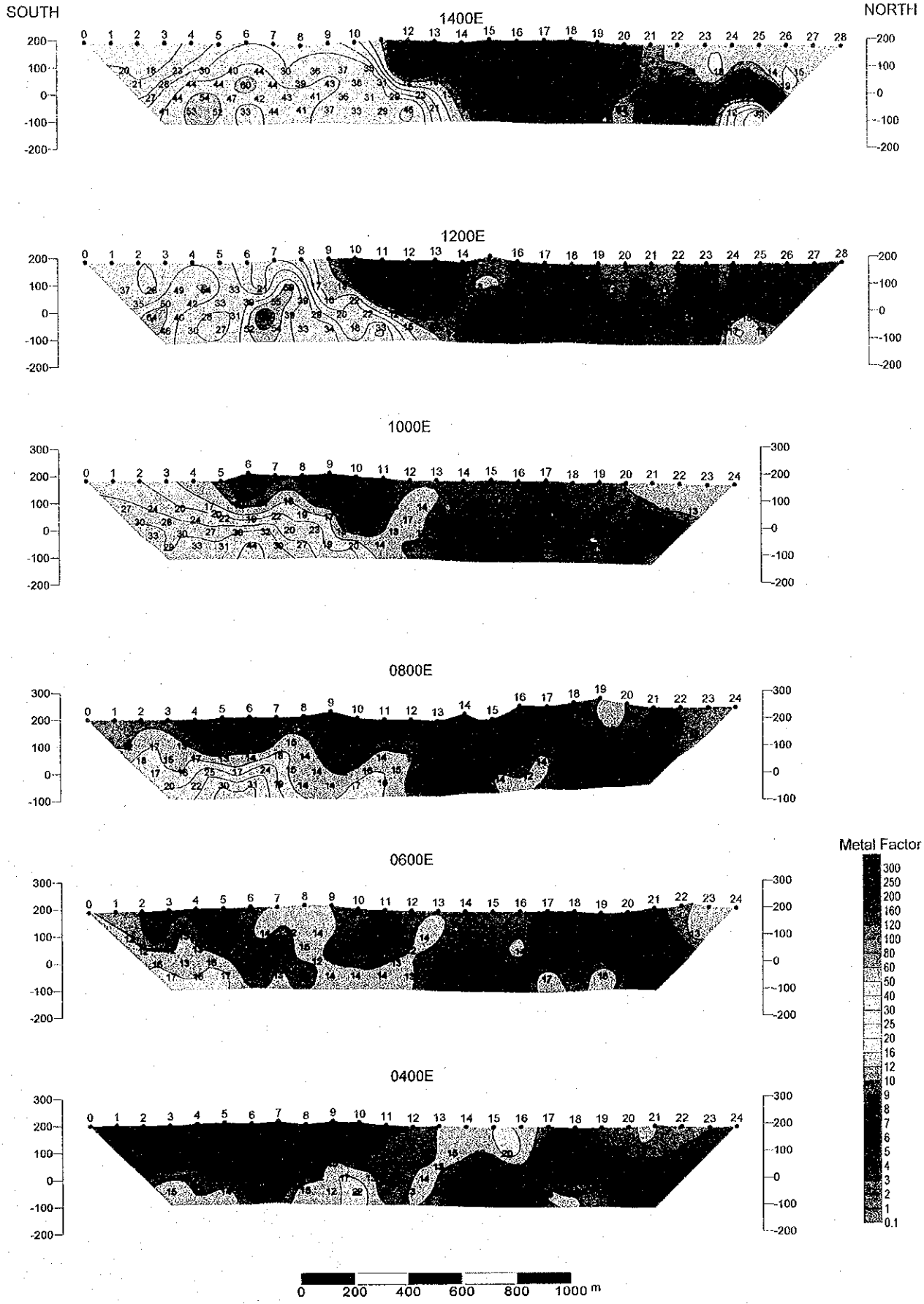

Fig. II -2-7(1) Metal factor pseudo-sections in Ghuzayn area(East)

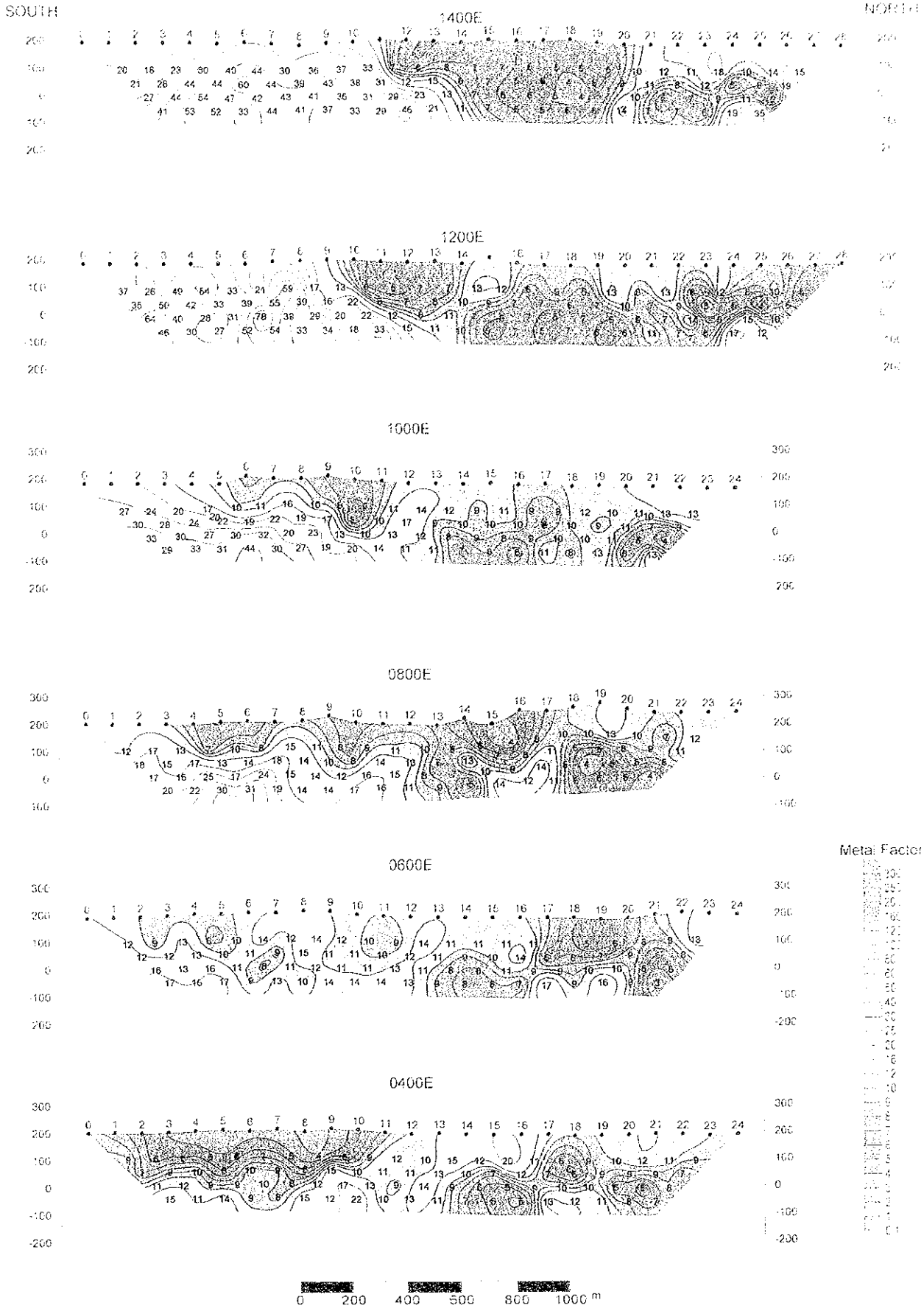

Fig. II-2-7(1) Metal factor pseudo-sections in Ghuzayn area(East)

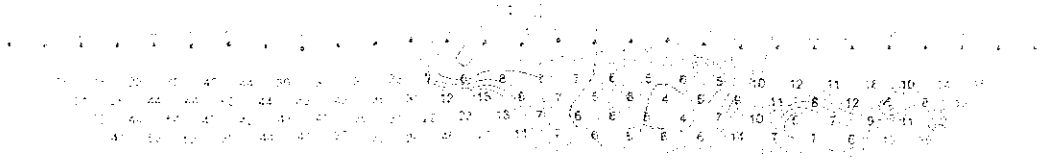

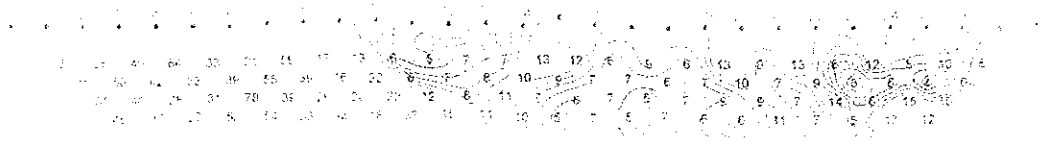

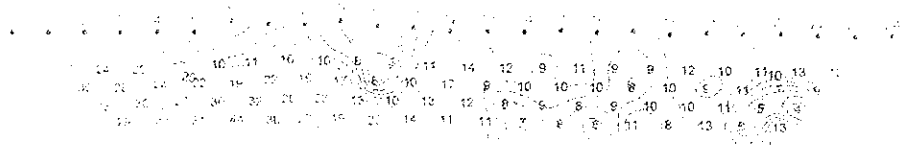

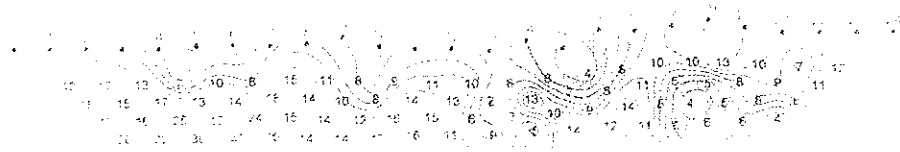

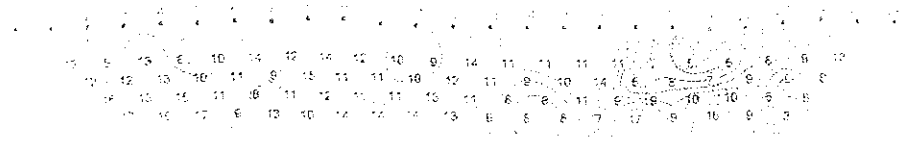

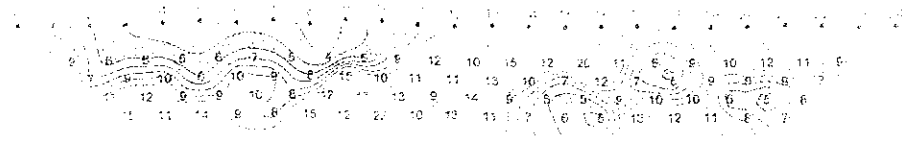

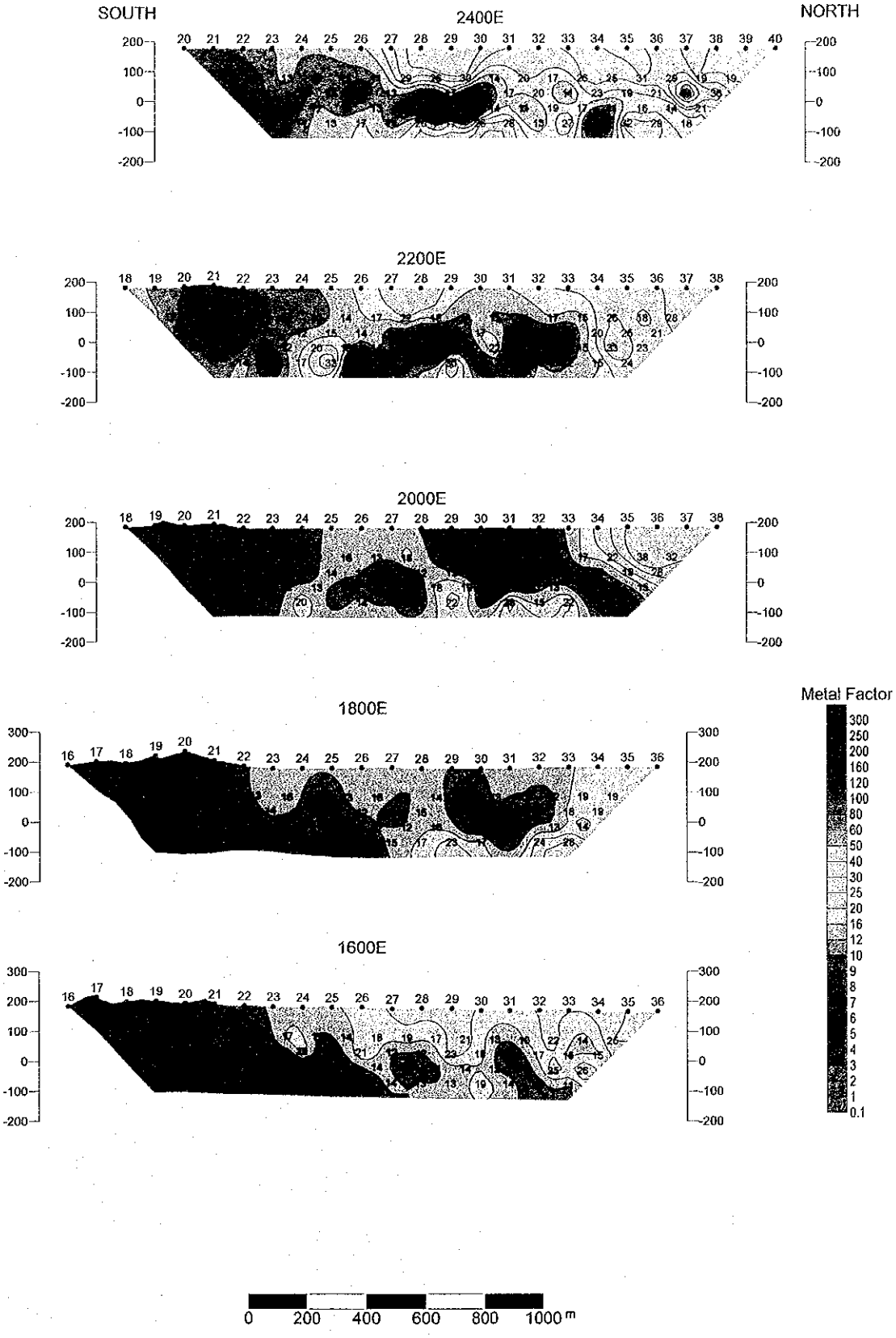

Fig. II -2-7(2) Metal factor pseudo-sections in Ghuzayn area(East)

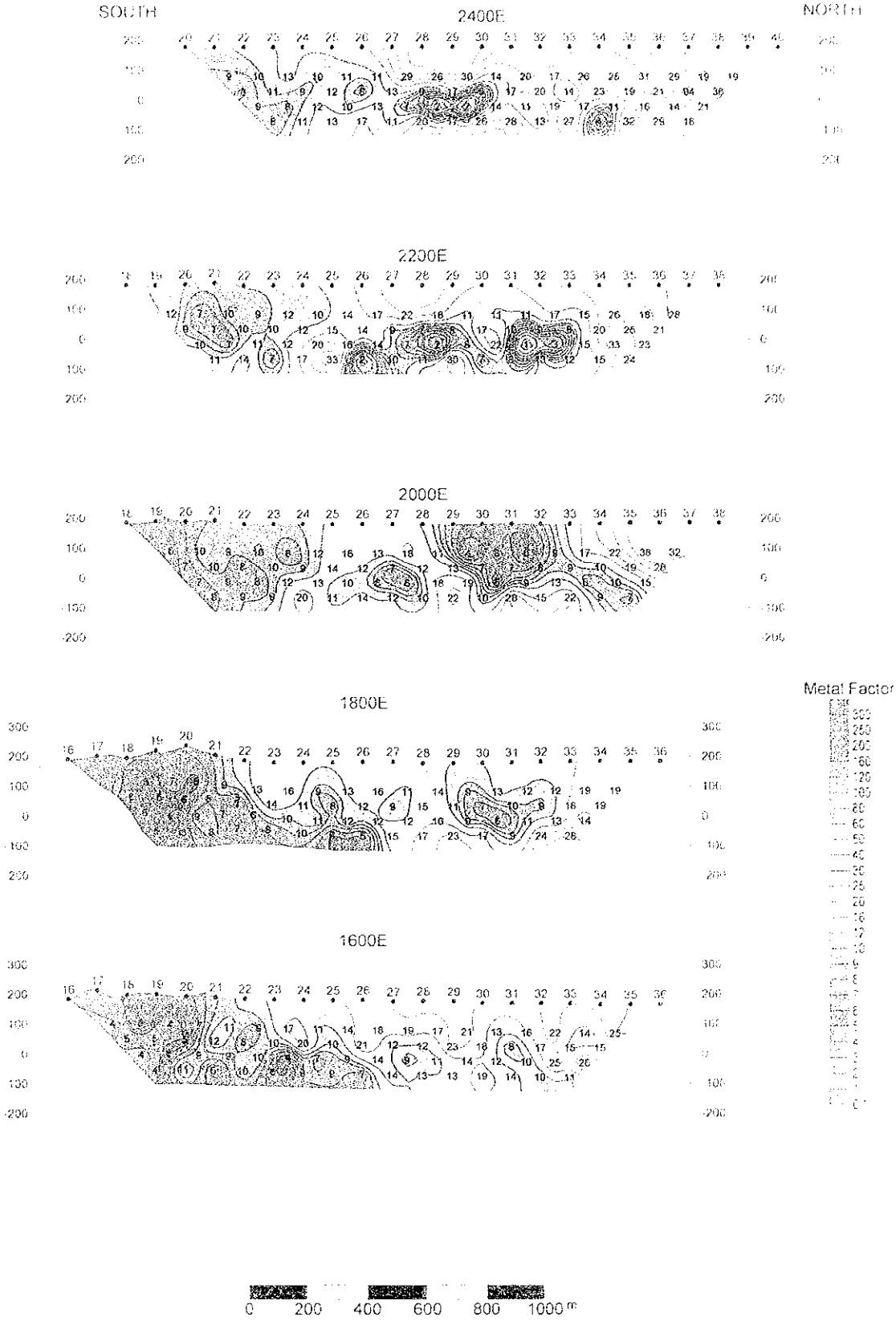

Fig. II -2-7(2) Metal factor pseudo-sections in Ghuzayn area(East)

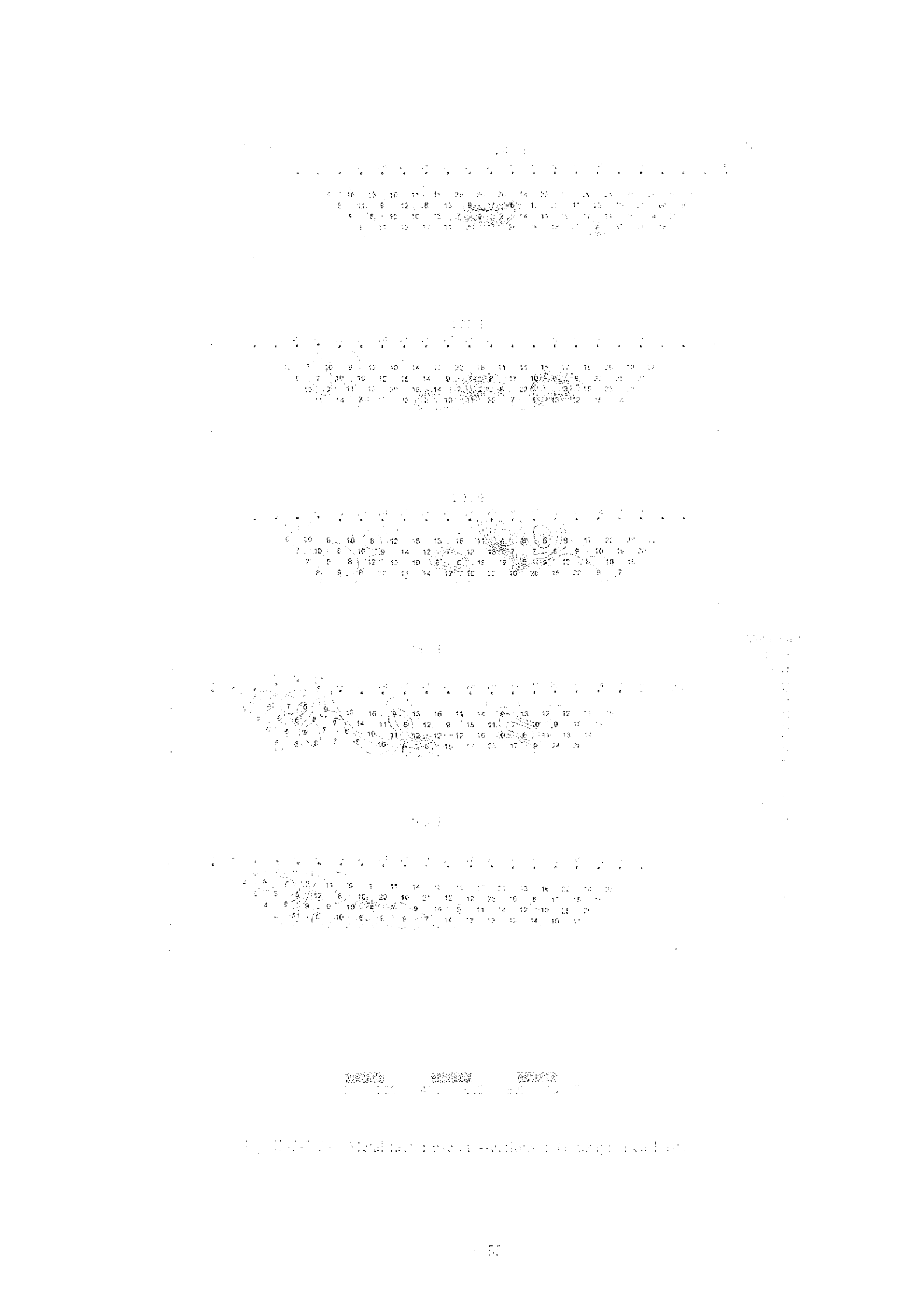

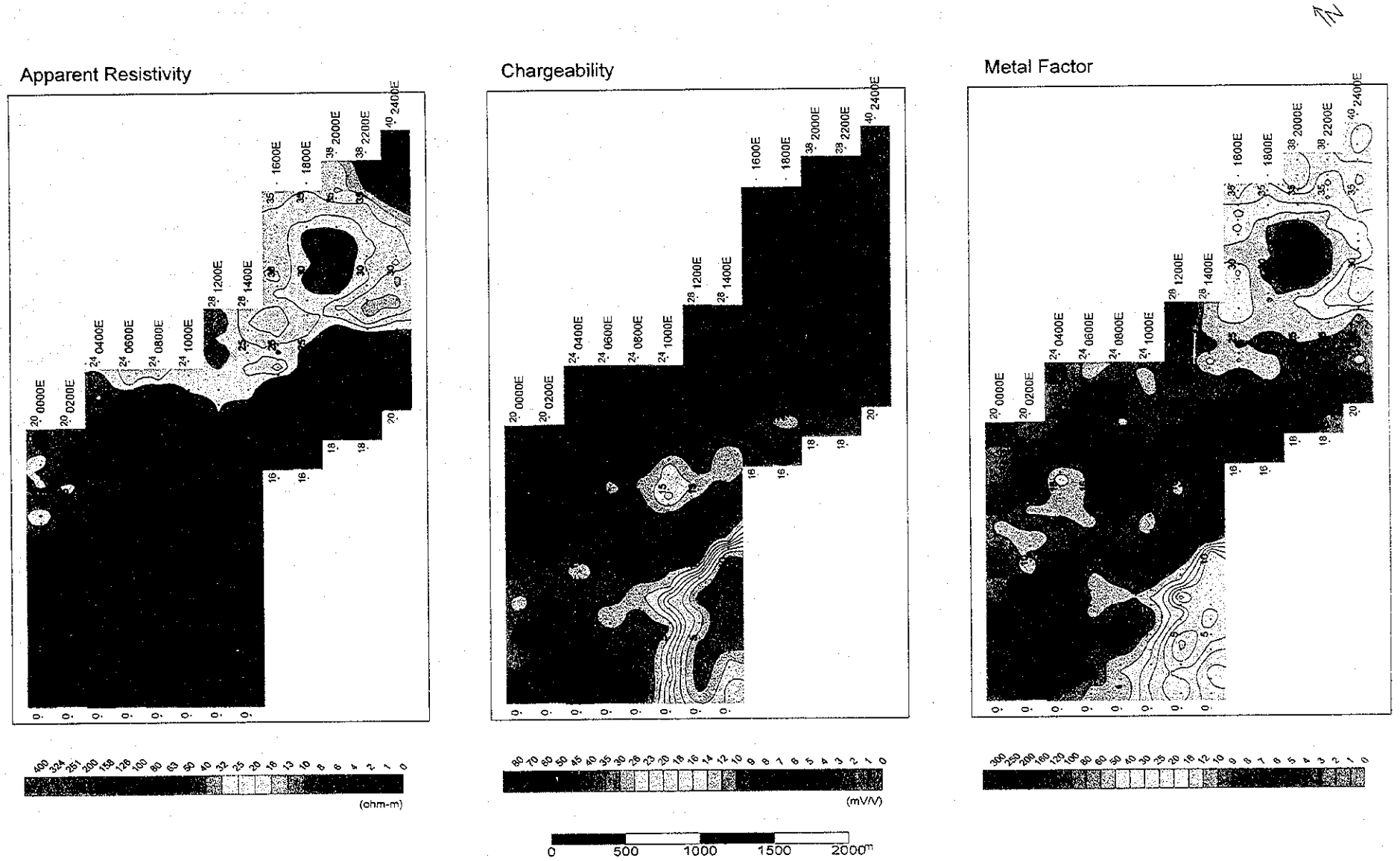

Fig. II -2-8 IP plane map of n=1 in Ghuzayn area(East)

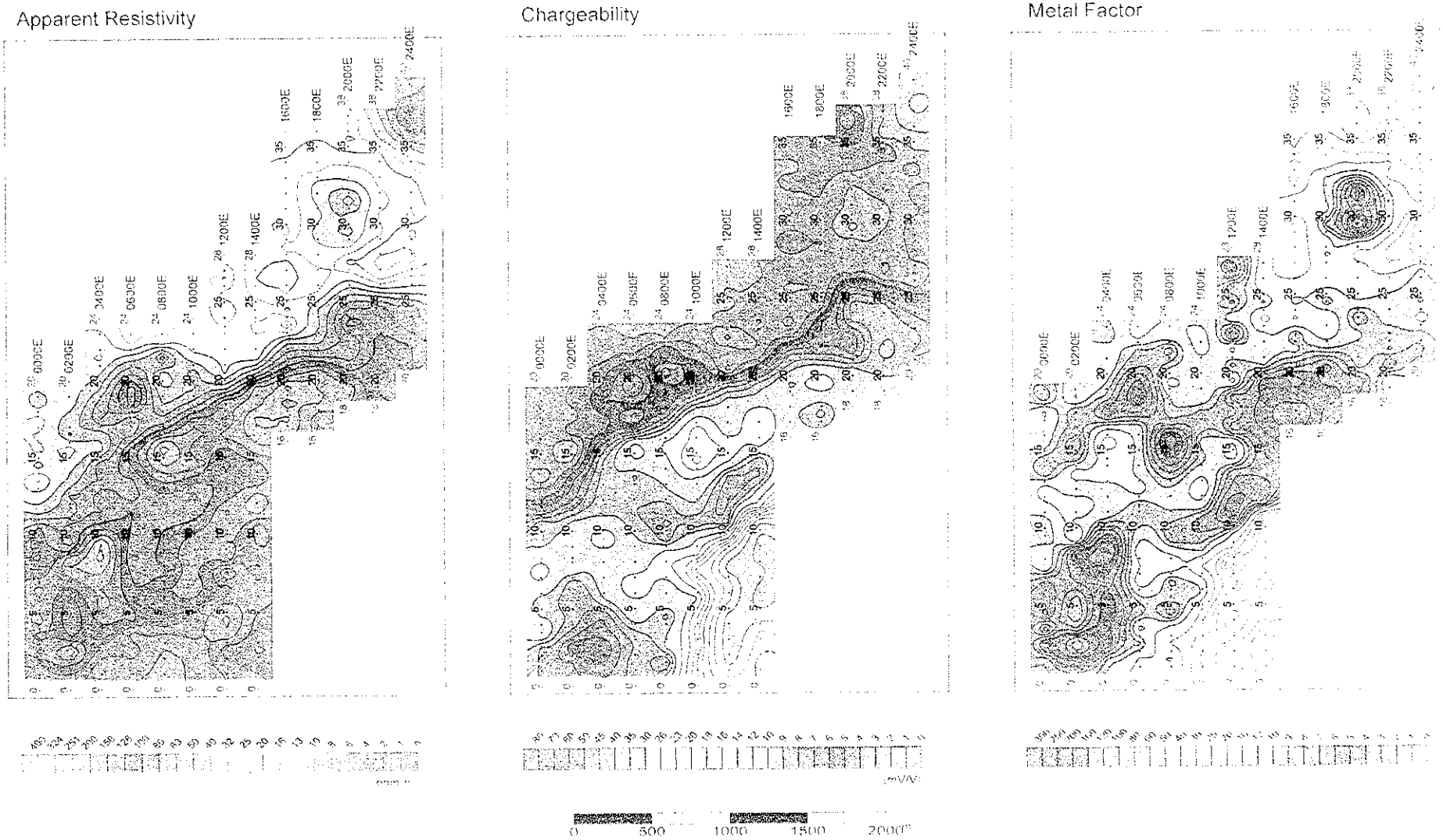

Fig. II-2-8 IP plane map of n=1 in Ghuzayn area(East)

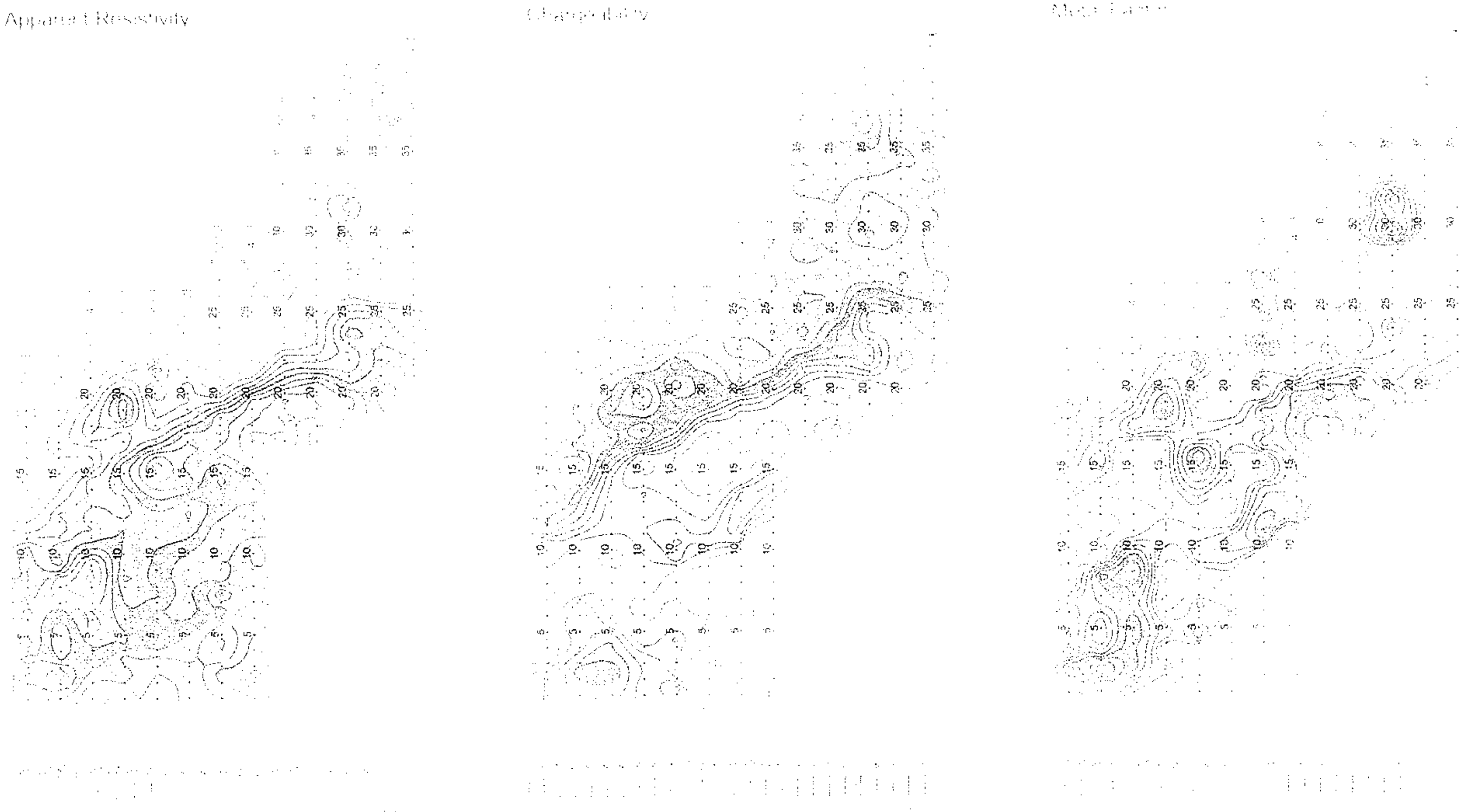
Apparent Resistivity
Chargeability
Metal Factor

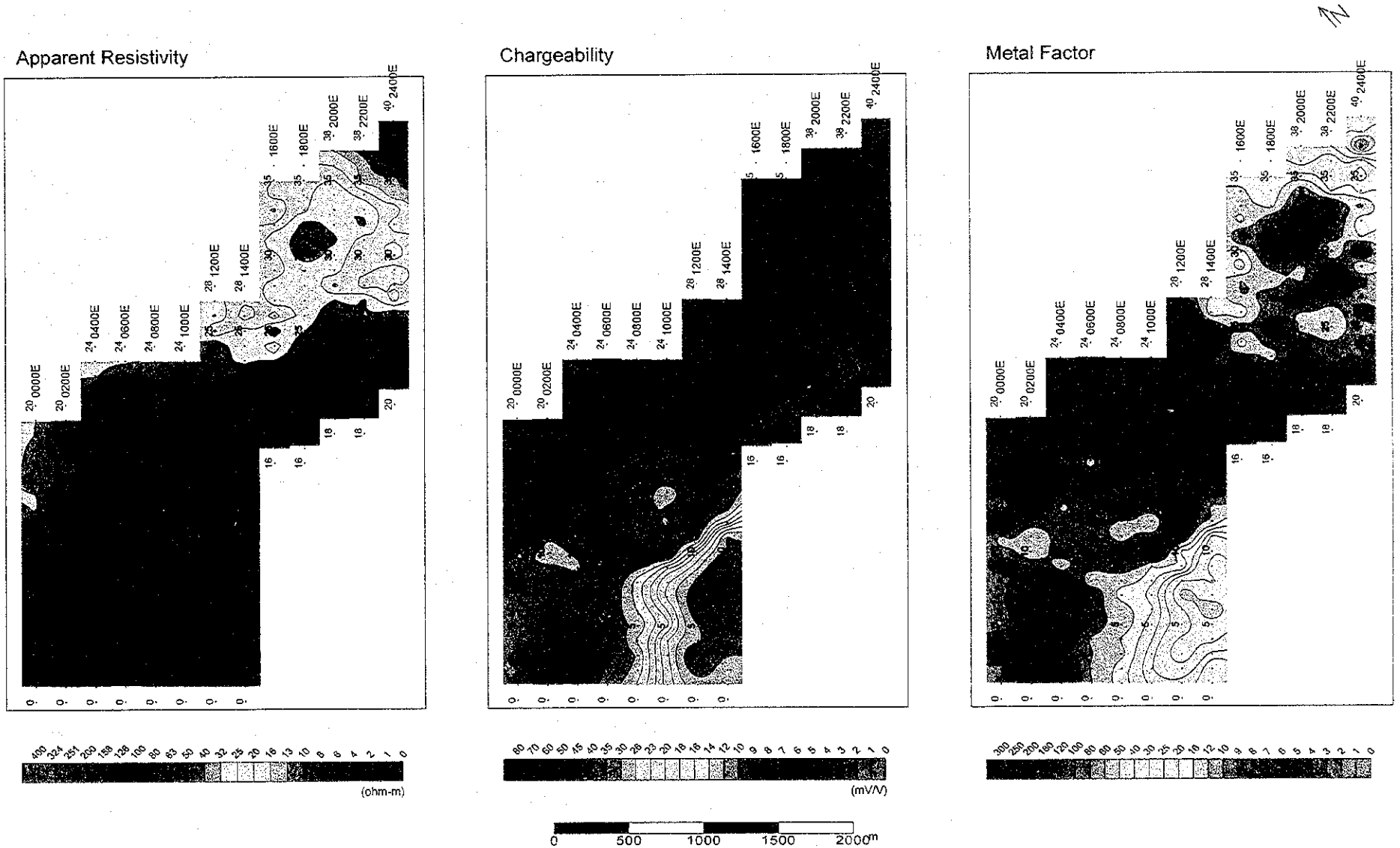

Fig. II -2-9 IP plane map of n=2 in Ghuzayn area(East)

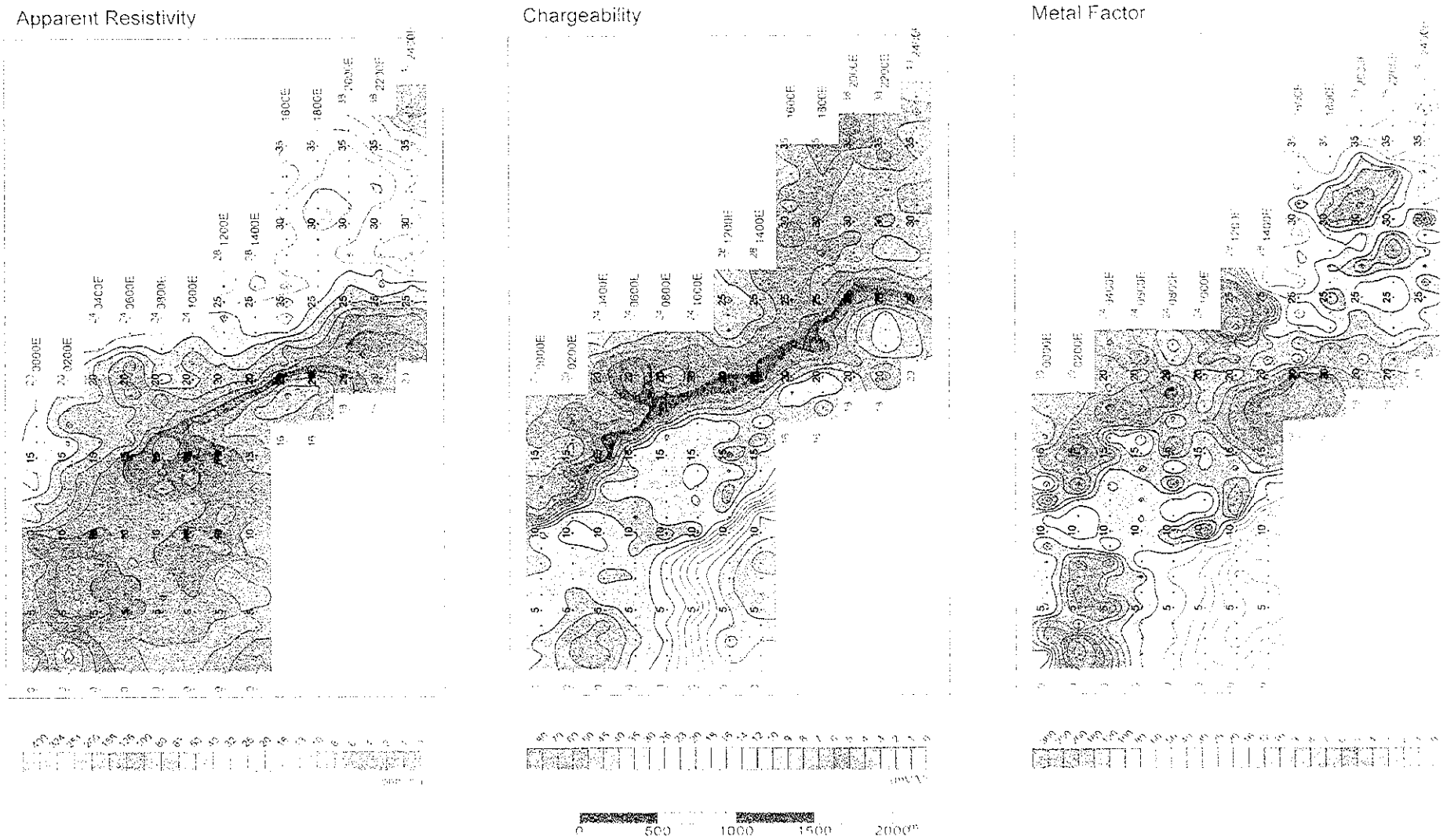

Fig. II -2-9 IP plane map of n=2 in Ghuzayn area(East)

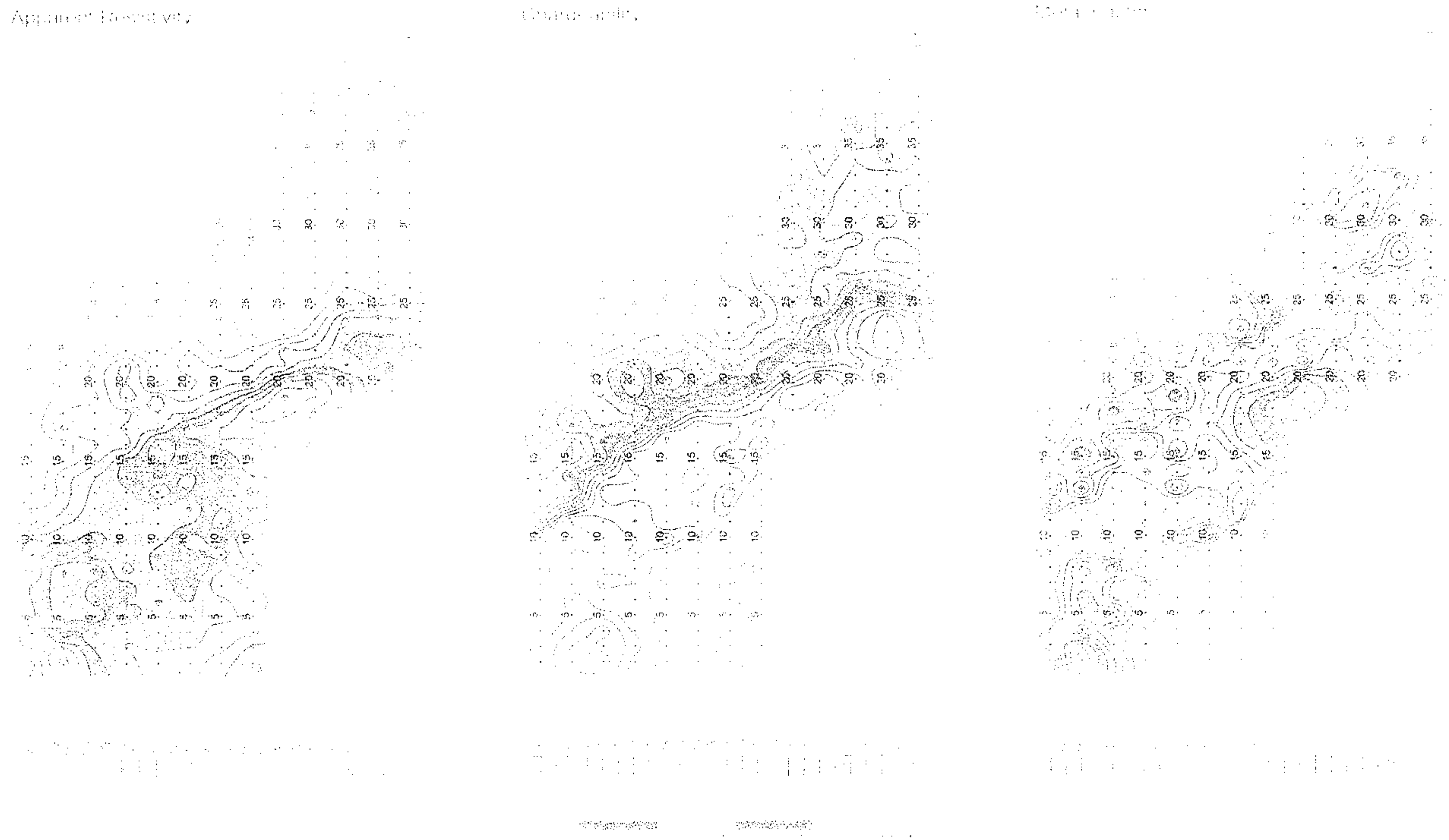
Apparent Resistivity
Chargeability